ADDIS ABABA UNIVERSITY

SCHOOL OF GRADUATE STUDIES

SOLID-STATE PHOTOELECTROCHEMICAL SOLAR ENERGY CONVERSION BASED ON BLENDS OF POLY(3-HEXYLTHIOPHENE)/FULLERENE AND POLY(PARAPHENYLENE) DERIVATIVE/FULLERENE

Ushula Mengesha

June, 2005

SOLID-STATE PHOTOELECTROCHEMICAL SOLAR ENERGY CONVERSION BASED ON BLENDS OF POLY(3-HEXYLTHIOPHENE)/FULLERENE AND POLY(PARAPHENYLENE) DERIVATIVE/FULLERENE

By

Ushula Mengesha

A Thesis

Submitted to the

School of Graduate Studies

Addis Ababa University

In Partial Fulfillment of

The Requirements for the Degree of

Master of Science in Chemistry

June 2005

ADDIS ABABA UNIVERSITY

SCHOOL OF GRADUATE STUDIES

SOLID-STATE PHOTOELECTROCHEMICAL SOLAR ENERGY CONVERSION BASED ON BLENDS OF POLY(3-HEXYLTHIOPHENE)/FULLERENE AND POLY(PARAPHENYLENE) DERIVATIVE/FULLERENE

BY

USHULA MENGESHA

DEPARTMENT OF CHEMISTRY

FACULTY OF SCIENCE

APPROVED BY:	SIGNATURE
Dr. Teketel Yohannes Advisor	
Prof. Theodros Solomon Chairman	
Dr. Mesfin Redi Examiner	
Dr. Ahmed Mustefa Examiner	

ACKNOWLEDGEMENTS

I offer my deepest gratitude and special affection to my advisor Dr. Teketel Yohannes for his generous advise, devoted assistance, encouragement in all stages of the work, constant guidance and constructive criticism which were necessary for the progress of the research. The convenient working environment he has created with the necessary materials is greatly appreciated. It is a great privilege to work with him.

I would like to express my thanks to all my friends for their encouragement, and Tigist Yohannes for her cooperation at all times of the work. Particularly I would like to express gratefulness to Ato Assefa Sergawie for the concern he has shown, and the suggestions and encouragement he has offered to me in problems which I have met in the work.

I am grateful to Bahir Dar University, which allowed me to continue my graduate studies. Finally, it is a pleasure for me to express my gratitude to the Department of Chemistry of Addis Ababa University for providing me with laboratory and other facilities needed for the accomplishment of this work.

TABLE OF CONTENTS

LIST OF FIGURES

LIST OF TABLES

Abstract

Solid-state photoelectrochemical cells(PECs) based on blends of conjugated semiconducting polymers and Buckminsterfullerene have been constructed and studied. The PEC contains a photoactive layer consisting of poly(3-hexylthiophene) (P3HT) or poly(2-methoxy-5-(3',7'-dimethyloctyoxyl)-1,4-phenylenevinylene) (MDMO-PPV) as electron donor and Buckminsterfullerene (C_{60}) as electron acceptor, an ion conducting polymer electrolyte containing amorphous poly(ethylene oxide) (POMOE) complexed with I_3^-/I^- redox couple and a counter electrode poly(3,4-ethylenedioxythiophene) (PEDOT) coated on indium doped tin oxide (ITO) coated glass. The photoelectrochemical properties of solid-state PEC using pure P3HT and pure MDMO-PPV as a photoactive layer were used for comparison. The effective area of the PECs studied was 1 cm^2. The constructed PECs have resulted in the following solar cell parameters: V_{oc} = 97.8 mV, I_{sc} = 7.28 μAcm^{-2}, FF = 0.26, IPCE = 0.43 % for blend of P3HT/C_{60}, and V_{oc} = 146 mV, I_{sc} = 0.171 μAcm^{-2}, FF = 0.25, IPCE = 0.012 % for blend of MDMO-PPV/C_{60} based PEC at incident light intensity of 100 mW/cm^2. Analysis of the photoelectrochemical properties of the cells showed that blends of P3HT with C_{60} and MDMO-PPV with C_{60} based PECs have better short-circuit current (I_{sc}) and incident monochromatic photon to current conversion efficiency (IPCE %) compared to that contained pure P3HT and MDMO-PPV. However, the open-circuit voltage (V_{oc}) and fill factor (FF) obtained showed better values for the pure P3HT and MDMO-PPV based PECs.

Keywords: Solid-state photoelectrochemical cell; Poly(3-hexylthiophene); Poly(2-methoxy-5-(3',7'-dimethyloctyoxyl)-1,4-phenylenevinylene); Buckminsterfullerene; amorphous poly(ethylene oxide); I_3^-/I^- redox couple; Poly(3,4-ethylenedioxythiophene) .

1. INTRODUCTION

A huge amount of research and technological application of solar energy utilization is carried out in converting light energy from the sun to electrical energy. The most important application of photovoltaic energy conversion in the past has been in space program. Today, however, the rising price of fuel, the realization that oil and gas supplies can only last a relatively few decades, and freedom of solar energy from pollution, have all led to closer look at solar energy as an alternative to present day fossil-fuel system [1].

Quite a number of research and development works on the use of solar cells have been made using inorganic semiconductors such as silicon as photovoltaic materials. But the use of these inorganic materials for electronic and optoelectronic devices requires high manufacturing cost. After the discovery that conductivity of conjugated polymer such as polyacetylene can be varied from insulating through semiconducting to metallic regimes [2], researches on the application of conducting polymers are being conducted to find an alternative to the conventional inorganic materials in many applications because their semiconducting properties, diversity and ease of fabrication, and potentially low cost.

Polymers are often considered as insulators. Although this is true for saturated polymers, the situation for conjugated polymers is different. In conjugated polymers the sp^2 hybridization leads to one unpaired electron which results in alternating single and double bonds along the backbone of the chain. This alternating single and double bonds (conjugation) is the origin of the interesting electronic properties of conducting polymers.

The first conjugated polymer tested as a semiconductor in a diode was polyacetylene [3]. But subsequent improvements in synthesis, stability, and processability have lead to numerous studies on polymeric diodes. Undoped or doped conjugated polymers, such as polythiophene and its derivatives have been studied as Schottky junction diodes [4,5], metal-insulator-semiconductor diodes [6], light emitting diodes [7], field effect transistors [8] and photoelectrochemical cells (PECs) [9-14]. There are also other conjugated polymers that

have been studied. All these studies have shown that these conjugated polymers do have semiconducting properties that can be used in device fabrications.

Recently derivatives of polythiophene and polyparaphenylene have attracted considerable attention because of their commercial availability, stability, processeablity, quality and ease of fabrication [10-12]. They are soluble in common organic solvents. Poly(3-hexylthiophene) (P3HT) and poly(2-methoxy-5-(3',7'-dimethyloctyoxyl)-1,4-phenylenevinylene) (MDMO-PPV) are one of the derivatives used as an active conjugated polymer for the devices that we studied. These polymers combine the commercial availability with sufficient solubility, a low band gap relative to the most conjugated polymer and a high degree of intermolecular order leading to high charge carrier mobilities.

Increasing efforts have been put into the development of different types of solar energy conversion devices based on organic molecules and polymeric materials. Unlike conventional inorganic solar cells, light absorption in organic solar cells leads to the production of excited bound electron-hole pairs commonly known as excitons. To achieve a substantial photovoltaic effect, the excited charge pairs thus produced need to be dissociated into free charge carriers through the assistance of an electric field or interface of materials with different electron affinities. Several approaches have already been adopted to achieve efficient exciton dissociation [9, 15-17]. So far, the method of blending conjugated polymers with high electron affinity molecules like C_{60} has turned out to be the most efficient way for rapid exciton dissociation resulting in solar cells with high power conversion efficiencies [17].

Organic photovoltaic solar cells with blends of conjugated polymers and fullerenes have been extensively studied. A less expensive solar energy conversion can be achieved by photoelectrochemical cells, which involve the use of semiconductor to absorb incident light and an electrochemical process at semiconductor/liquid junction to allow energy conversion. Organic PEC grab increasing research attention recently is the solid-state PECs with the ion conducting solid polymer electrolyte. These cells compared to liquid electrolyte PECs possess advantages such as handling, portability and packing. Previous studies on the solid

state PECs were focused on use of pure conjugated semiconducting polymer [12-14], and co-polymers [18] as photoactive electrodes.

Solid state photoelectrochemical solar cell based on conjugated polymer mixed with fullerene as a photoactive electrode has not yet studied except for some preliminary investigation. The use of conjugated polymer/C_{60} blends as photoactive electrodes give ultrafast electron transfer from optically excited polymer to C_{60}, resulting in improvements of photocurrent [19]. The aim of this work is thus, to construct solid-state PECs consisting of blends of conjugated semiconducting polymer and fullerene as photoactive electrode, and ion conducting solid polymer electrolyte complexed with a redox couple. The constructed devices were investigated using optical and photoelectrochemical measurements.

2. LITERATURE REVIEW

2.1. Conjugated Polymers

Polymers are macromolecules consisting of a great number of repeating units, which are coupled to each other by covalent bonds to form a long chain. These repeating units can be any group of atoms, however, we consider only organic polymers, where the backbone consists of only carbon. Most organic polymers that have side chains are soluble in organic solvents. The solvents easily evaporate upon spin coating or solvent casting, leaving thin films on a substrate [20].

Polymers in their neutral form are insulators due to the large band gaps and strong electron-phonon coupling, which are characteristics of these materials [21]. They are often considered uninteresting from electronic point of view until 1970's [22]. They were only used commonly for plastic bags, paints, adhesives, cloth and insulating electrical materials. Although this is true for polymers, which contain saturated carbons in which their backbone consist of sp^3 hybridized orbitals, the situation in conjugated polymers is much more interesting. In fact the conjugated structure is the origin of the interesting electronic properties of conjugated polymers. Their backbone consists of sp^2-hybridized carbons and show semiconducting properties.

The most interesting properties of organic materials arise from the delocalization of π-orbital. That is, the electrons in the π band are not concentrated along an axis between the two atoms but are shared in a region of space both above and below the plane defined by sp^2 orbitals. These molecules have strict alteration of single and double bonds. Double bonds are strong, localized and shorter where as single bonds are weak, delocalized and long. Due to strong and localized nature of double bonds, conductivity of conjugated polymers along the chain is very small, leading them to be insulators or semiconductors. There exist different kinds of conjugated polymers out of which some are depicted in Fig. 2.1.

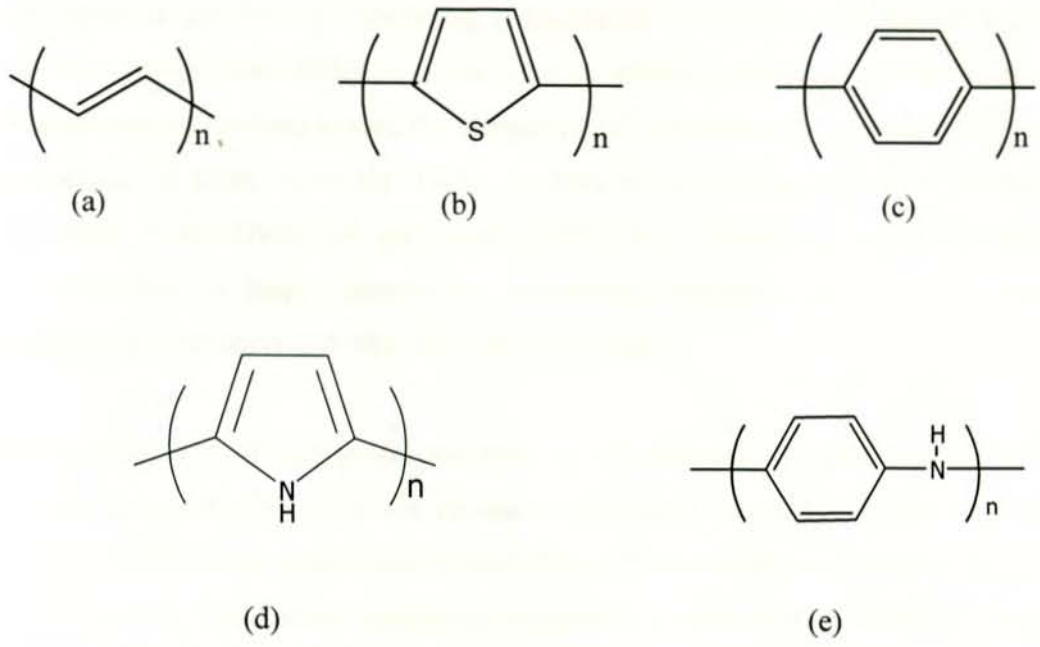

Fig. 2.1. Chemical structures of some conjugated polymers, (a) *trans*-polyacetylene, (b) polythiophene, (c) poly(*p*-phenylene), (d) polypyrrole and (e) polyaniline

Because they had the important electronic and optical properties of semiconductors and metals, conducting polymers became potential materials for technological applications. Conducting polymers became so popular and they are now the main topic in international conferences and meetings on synthetic metals. Several reviews have been published covering many different aspects of these materials [23-25].

2.2. Electrical Properties of Conjugated Polymers

Although the idea of using polymers for their electrically conducting properties dates back to the 1960's, the field really started with the discovery in 1977, when Shirakawa in Japan with his coworkers made polyacetylene conducting [2]. The partial oxidation with iodine or other reagents made polyacetylene films 10^9 times more conductive than they were originally thought. Since then, the dream of combining the processing and mechanical properties of polymers with their electrical and optical properties has driven both the science and technology of conducting polymers [26].

The work in the field of conducting polymers has become highly interdisciplinary with people coming from different areas such as physics, chemistry, material science and engineering all working toward the common goal; controlling the electrical and mechanical properties of these materials. Early research of conducting polymers focuses on the electrical conductivity of polymers. After the discovery of the conductivity of polyacetylene, a large number of conducting polymers that include aromatic and heterocyclic polymers and their derivatives are added.

The conductivity of conjugated polymers can be enhanced to higher levels by doping the neutral polymers. Doping is the process of changing the oxidation state or reduction of conjugated polymers with a concomitant change in the electronic properties of the material. Although the term doping is applied to conjugated polymers, it is different from that of the conventional semiconductors. In semiconductors the dopant species occupy positions within the lattice of the host material, resulting in the presence of either electron-rich or electron deficient sites, with no charge transfer occurring between the two species. The doping reaction in conjugated polymers is essentially a charge transfer reaction resulting in the partial oxidation or reduction of the polymer, rather than the creation of holes or electrons [27].

In the language of semiconductor physics, the partial oxidation of conjugated polymers is referred to as p-doping and the partial reduction is referred to as n-doping, but the basic process is the removal of electrons in the first case and gain of electrons in the latter case. The doping processes can be represented as shown below:

For p-doping: $\text{Polymer} + X \rightleftharpoons (\text{Polymer})^{n+} + X^{n-}$

For n-doping: $\text{Polymer} + M \rightleftharpoons (\text{polymer})^{n-} + M^{n+}$

where X is the oxidizing agent and M is the reducing agent. X^{n-} and M^{n+} are the dopant anion and cation, respectively [28].

Conjugated polymers can be doped either chemically or electrochemically. However, electrochemical doping is emerging as the preferred technique in many applications because it provides a potentially high controllable and reproducible method for investigation of the doping process in which the transfer of charge can be accurately monitored and regulated giving a degree of control which is beyond the scope of gas or solution phase chemical doping [27].

2.2.1. Charge Carriers

In conventional inorganic semiconductors, conductivity is due to the presence of electrons and holes. In conducting polymers the conductivity is due to defects in conjugation. There exist two energetically equal forms of polyacetylene in its ground state, Fig. 2.2 (a, b). If the two phases exist in the same chain, there will be a defect, which separates the bond alteration, as shown in Fig. 2.2 (c). This defect is usually called soliton [29-31]. Since the chain is energetically equal the solitons can move freely along the backbone of polymer polyacetylene. A single soliton in polyacetylene can be accommodated per fourteen carbon atoms along the chain [32]. Solitons conserve charge and energy as water waves conserve shape and energy [33]. But there is a difference in passing through each other, water waves can pass through while solitons in polymers cannot.

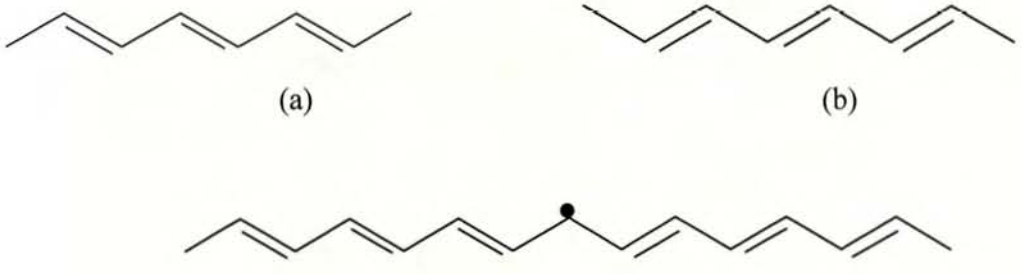

Fig. 2.2. (a) and (b) are two energetically equal structures of polyacetylene, (c) is the formation of a soliton due to a misfit of the two structures in a single chain.

These defects (solitons) are neutral since the carbon atom at the soliton site is electrically neutral. This soliton is a dangling (unbounded) electron. It produces a new electronic state

at the band gap. This state carries a reversed spin-charge relationship. Solitons can be generated by means of chemical, electrical, exposure to light or charge injection.

During doping the defect is more sensitive than the rest of the chain. In the process of doping, if two electrons compensate the carbon ion, the defect (soliton) will be negatively charged. On the other hand if no electron compensate the carbon ion, it will be positively charged. In such cases the defects are called negative soliton or positive soliton, respectively, as shown in Fig. 2.3.

Doping conjugated polymers will create states in the forbidden gap. If the doping level increases, the electronic states within in the gap will form soliton band. At about 30% of doping level these states expand and fill the gap resulting in the metallic conductivity [21]. Electronic states formed within the gap by these three types of defects, i.e., neutral, negatively charged, and positively charged, are illustrated below in Fig. 2.4.

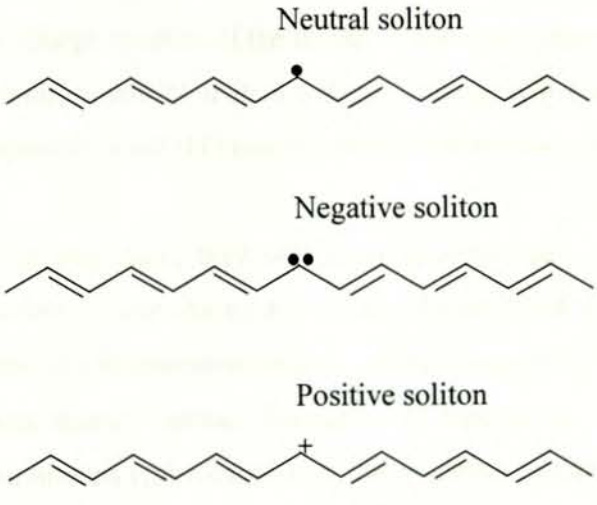

Fig. 2.3. Solitons in *trans*-polyacetylene.

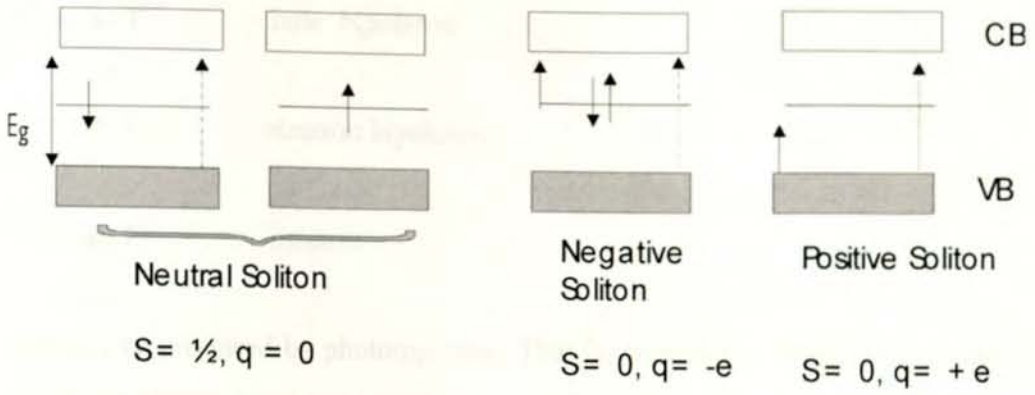

Fig. 2.4. Schematics of the energy band diagram of polyacetylene with solitons. Dashed and thin solid arrows indicate the interband and sub band transitions, respectively, where as the short arrows represent electrons spins.

To create defects in non-degenerate polymers, we should have double bound defects called polarons. Here one of the defects must be neutral while the other is charged negatively or positively. If the other is negatively charged the bound defect will be an electron polaron, where if it is positively charged it will be a hole polaron. These charge carriers are generally formed from charge transfer. If the dopant is acceptor, charge transfer takes place from polymer to acceptor, where as if it is a donor, charge will transfer from dopant to polymer. Here an acceptor (A^-) and (D^-) counter ions reside between polymer chains.

If two polarons exist in one chain, they will move towards each other to minimize the energy and form bipolarons. Here the neutral defects interact and form a bond while the charged solitons remain at a minimum separation of four rings [34, 35]. So bipolarons are doubly charged spinless charge carriers. Formation of bipolarons is due to the fact that formation energy of bipolarons is favorable over the existence of two polarons, i.e., energy of the two polarons is greater than energy of bipolaron ($E_b < E_p$, where E_b is energy of bipolarons and E_p is energy of polaron) [36]. If two of the defects are positive, the existing doubly charged defects are hole polarons, where as if both of them are negative, it will be electron bipolaron. There is a considerable possibility that an electron and a hole polarons interact to yield a bound electron-hole pair called an exicton see Fig. 2.5.

$P^+ + P^+ \longrightarrow P^{++}$ hole bipolaron

$P^- + P^- \longrightarrow P^{--}$ electron bipolaron

$P^+ + P^- \longrightarrow P^{-+}$ exicton

Excitons can be produced by photoinjection. That is, an incident photon is absorbed by an electron in the valence band and jumps to the conduction band leaving a hole in the valence band. These electron-hole pairs in polymers created as a result of photon absorption are bounded together. This mechanism is photogeneration of charge carriers. Bipolarons may be formed directly in addition to recombination of two polarons at high doping level.

Polarons and bipolarons create two interacting states within the forbidden energy gap [37]. These two states are symmetric with respect to the gap center. The presence of new electronic states in the band gap makes new electronic transitions possible as shown in Fig. 2.6.

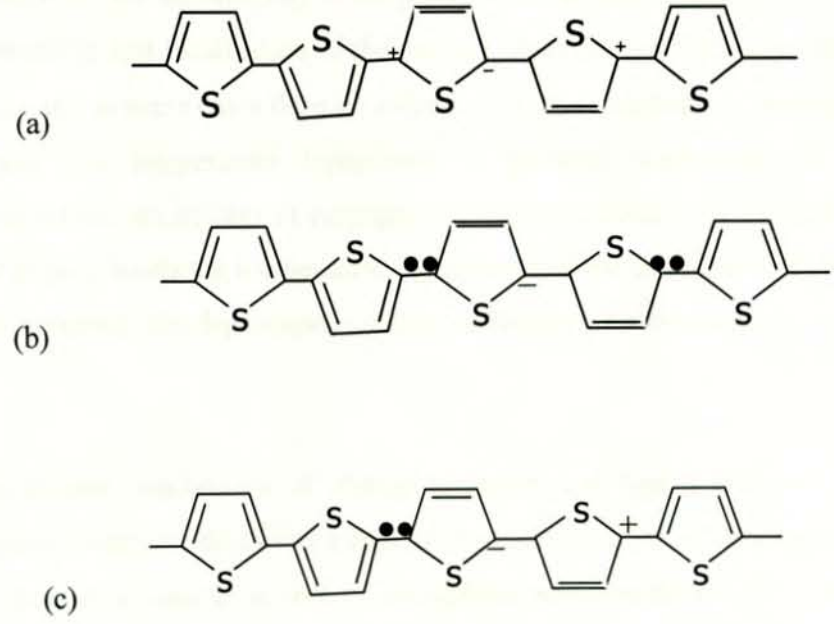

Fig. 2.5. (a) Hole bipolaron, (b) Electron bipolaron (c) Exciton

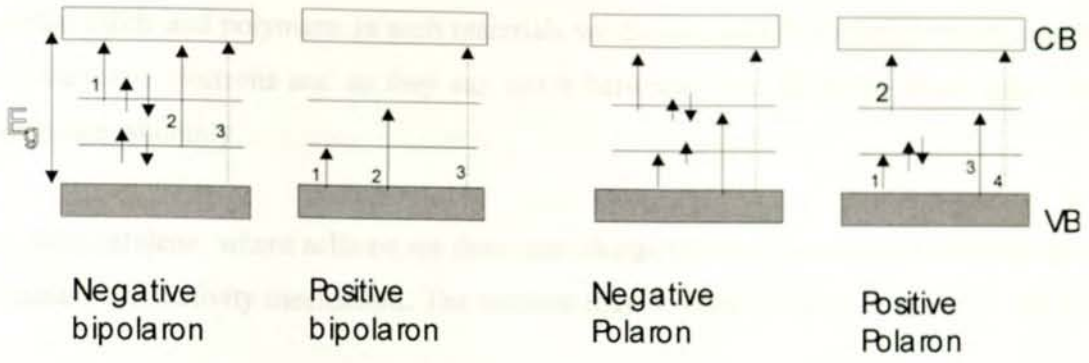

Fig. 2.6. Energy band diagrams showing polaron and bipolaron states in the non-degenerate polymer. The arrows indicated by the numbers 1, 2, 3, and 4, represents the possible optical transitions.

2.2.2. Charge Transport Mechanism

The prerequisite for charge transport is the presence of mobile charge carriers. In conducting polymers the conductivity is the presence of solitons, polarons and bipolarons, which are formed by self-localization of the carriers, induced into the π electronic systems through doping and in some cases during synthesis [38]. Conductivity of materials depends on temperature. The temperature dependence of polymer conductivity is manifested opposite to that of metals. In case of conjugated polymers conductivity depends on doping level. At low doping levels the temperature dependence of the conductivity is high. As the doping level increases, the dependence of the conductivity on temperature becomes less [39].

There is no definite mechanism of charge transport and hence different models are suggested over the whole conductivity range. In the undoped form of conjugated polymers, the charge transport is similar to that of amorphous semiconductors. It is explained by hopping between localized states. At very low doping levels, the conductivity is mainly due to hopping (phonon assisted quantum mechanical tunneling). Its concept is generally deduced from ionic conduction to electronic conduction in amorphous and disordered non-

metallic solids and polymers. In such materials we do not have free charge carriers, rather than localized electrons and so they can move between these localized states which are distributed randomly.

For polyacetylene, where solitons are dominant charge carriers, intersoliton hopping is the dominant conductivity mechanism. The solitons may be either neutral or charged, see Fig. 2.7.

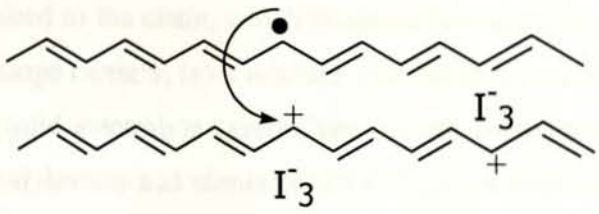

Fig. 2.7. Intersoliton hopping in *trans*-polyacetylene [21].

The charged solitons are trapped by the dopant ions and neutral solitons are free to move. When neutral soliton passes close by a charged soliton, an electron can hop between the mid gap states belonging to the solitons [40].

2.3. Polymer Electrolytes: Ionic Motion in Polymers

While electronic conductivity is the phenomenon related to the electrons-holes movement into solid conductors, ionic conductivity is described as the charge movement due to the ions motion. As the first applications regarding the electrical properties of polymers were directed to their insulating characteristics, ionic conduction in polymers was initially observed as an undesired property. However, this point of view changed in the 1970s when Wright and co-workers carried out the pioneering measurements of ionic conductivity in polymer-salt mixtures [41]. Since that time, the research on solid polymeric electrolytes has grown intensely and reviews with historic surveys have been published [42, 43]. The interest in these solid-state ionic conductors comes from the possibility of using them to substitute the liquid electrolytes in several electrochemical devices. The major challenge into replacing the liquid or gel electrolyte by a polymeric one is to keep the high operation efficiency,

similar to the electrochemical devices based on liquid junctions. Besides improving the stability of the active interface, allowing a long-term durability, a polymer electrolyte eliminates problems concerning evaporation or leakage of the solvent.

The use of polymer in electrolytes can be divided in three categories, as follow: (a) a polymer swollen with a liquid electrolyte, which provides high values of conductivity, but does not eliminate the problems related to the liquid electrolytes; (b) a polymer containing cations or anions attached to the chain, which produces low conductivity values because of the low mobility of charge carriers; (c) a mixture of a salt in an ion-solvating polymer, that configures a dry and solid electrolyte system, can present conductivity values suitable for using in electrochemical devices and eliminates all difficulties relative to the use of liquid or gel electrolytes in commercial applications.

The thermodynamics involved in dissolution of a salt into a polymer matrix is the same as observed in liquid solvents. In a simple analysis, the entropy favors the dissolution since the salt dissociation provides the increase in the number of particles in the system and, consequently, the increase of the system entropy. Differences observed by dissolving several salts in the same polymer are related to the lattice enthalpy of the salt, cohesive enthalpy of the solvent and solvation energy. Thus, the dissolution and dissociation of a salt into a polymer matrix will be more effective if the salt has low lattice energy, the solvent has a low cohesive enthalpy and high solvation energy [44]. Considering these statements, polar solvents are the ideal candidates for dissolving a salt. After dissociation, cations act as Lewis acids and interact with electron donors sites (Lewis bases) in the polymer chain. Otherwise, the anions have Lewis base character and interact with electron acceptor sites (Lewis acids) in the polymer.

Poly(ethylene oxide), PEO, is the reference polymer for ionic conduction, since it is the best matrix for alkali salts because of the high Lewis base character of the oxygen atoms present in this polyether. Due to this reason, great efforts have been devoted to make polymer electrolytes based on PEO, combining it with several salts [45-47].

Several hypothesis have been proposed to explain the ionic motion in PEO chains. The first solid electrolyte systems were based in crystalline non-processable materials, such as Li_3N, AgI and β-alumina [48]. In analogy to these inorganic conductors, the ionic conductivity in PEO was initially associated to its crystalline phase. Conductivity measurements of PEO-salt complexes at several temperatures showed a large increase above the melting temperature of the polymer [49]. Besides, ionic conductivity is not significant below the glass transition temperature of its amorphous phase. Taking into account these observations, the ionic conductivity in semicrystalline polymer-salt complexes was assigned to the segmental motion of the amorphous phase of the polymer chains [50]. Thus, the conductivity pathway was attributed to the amorphous part of the polymeric matrix, assisted by the segmental motion of the polymeric backbone, and the additional possibility of simultaneous coordination of one metallic cation to several Lewis base sites because of the flexibility of the polymer chains.

This theory has been accepted from the 1970's and, until very recently, no studies were devoted to contradict it. However, a very recent work showed that, in contrast to the prevailing view, ionic motion in polymer systems could be higher in the crystalline phase than that observed in the amorphous phase [51]. In this interesting work, the results indicated that ionic conductivity occurs preferentially in the crystalline phase of the PEO-salt complex at temperatures ranging from the glass transition temperature of its amorphous phase to the melting temperature of its crystalline domain. However, ionic conductivity values in this temperature range are very low in comparison to those observed above the melting temperature. These interesting results open new perspectives to find new solid electrolyte systems, however, this recent model still does not explain the significant increase of the conductivity above the melting temperature, when the organized crystalline phase disappears.

Independent on the theories used to explain the ion motion; experimental results always show that PEO-based electrolytes show reasonable ionic conductivity for using in commercial electrochemical devices only above its melting temperature, precluding its application at ambient temperature. Thus, several strategies have been used to decrease the

crystallinity of PEO and improve the conductivity of its complexes at room temperature, such as: the addition of plasticizers, the use of PEO based blends [52, 53] or the preparation of copolymers [54].

An alternative is the use of mixtures of PEO with different acrylic polymers [52]. The blends-salt complexes showed higher ionic conductivity in comparison to the pure PEO-salt complexes. This effect was not only assigned to the lowering of PEO crystallinity in the blends, but also to the presence of a highly flexible amorphous phase and the cooperative effect of polar groups on ionic transport.

Nowadays, new electrochemical devices are in development, making necessary the study of polymer electrolytes with special requirements [55, 56]. For using it in an electrochromic device, for example, the polymer electrolyte film should also posses high transparence to enhance the chromatic contrast of the entire device. Otherwise, mass transport takes place faster in electrochromic devices. Additionally, a photoelectrochemical cell needs an electrolyte containing a redox couple to transport to the counter electrode the photogenerated charge carriers.

The polymer electrolyte used in this study is amorphous poly(ethylene oxide), POMOE, with a repeating unit of $CH_2(CH_2CH_2O)_9$. It is known to have very good ionic conductivity at room temperature [57, 58]. The redox couple used to complex with the polymer electrolyte is iodine/triiodide.

2. 4. Fullerene

The new carbon allotropes, the fullerenes, are closed-cage carbon molecules with three-coordinate carbon atoms tiling spherical or nearly spherical surfaces. The best known of these molecules is Buckminsterfullerene, C_{60}, which has sixty carbon atoms forming a truncated-icosahedral structure with twelve pentagonal rings and twenty hexagonal rings, as shown in Fig. 3.1. The structure is essentially that of the soccer ball. The coordination at every carbon atom is not planar but rather slightly pramidalised at every carbon atom. In

other words some sp^3 character is present in the essentially sp^2 carbons of fullerenes. The structure of C_{60} can be visualized as being obtained by spacing apart the pentagons of the pentagonal dodecahedron with hexagons.

Because of their rich π-electron structure, fullerenes display complex electro-optical properties. These constitute important applications for fullerenes and fullerene-based materials. Some exciting applications of the fullerenes involve their properties as dopants and charge acceptors in polymeric systems.

The Buckminsterfullerene, C_{60}, was used as an electron accepting material in this work. Its electron accepting properties due to ultrafast charge transfer has been extensively studied [59]. Besides having a high electron affinity, C_{60} is fairly transparent and also has fair electron conductance (10^{-4} S cm^{-1}). This makes fullerenes a good component in photovoltaic cells.

2.5. Photovoltaic Energy Conversion using Conducting Polymers

In photovoltaic energy conversion, the solar cell converts light energy directly into electrical energy. The materials which are used for this purpose are classified as semiconductors. A tremendous research and development was made in enhancing efficiency and practical application of solar cells using inorganic semiconductor materials such as silicon, gallium arsenide, sulfide salts of cadmium and copper, and other alloys of these materials. Research work on polycrystalline and amorphous silicon is still active. Moreover, organic semiconductors and conjugated polymers have been also used in devicing the solar cells. The similarity of their electrical and optical properties to the inorganic semiconductors makes the polymers an alternative for electronic and optoelectronic devices. Polymeric materials can be considered as *n*-type and *p*-type semiconductors. Thus, in the use of these materials for solar cell devices, Schottky barrier theory as developed for inorganic semiconductors, can be applied to them. As far as inorganic semiconductor is concerned the most popular junction in electronic industry is the *p-n* junction, most of the organic diodes are based on another structure, the metal- semiconductor or Schottky barrier junction.

Although it is possible to construct the *p-n* junction of organic diodes, it is not stable yet. The main source of the instability of a *p-n* organic diode is the great ability of doping impurities diffuse from the p-to-n side (and vice versa) [60].

Photovoltaic effect in the rectifying Schottky junction can be explained as follows. The absorption of photon energy greater than the band gap results in the generation of electron-hole pairs or the absorption of a photon creates an exciton rather free charge carriers [61]. The photovoltaic current in the cell is then a direct transport of the free carriers in the first case while in the second case, in order to generate photocurrents, the excitons must dissociate into electrons and holes either in the bulk of the organic polymer or metal-polymer interfaces. In general the sequence that leads to a photovoltaic effect in organic polymer solar cell device can be described by simple four steps as follows [61, 62]: photogeneration of charges, charge separation, charge transport and charge collection to yield current.

2.6. Photoelectrochemical Solar Energy Conversion

2.6.1. Introduction

Photoelectrochemical cells are known for converting solar energy. These devices are simple to construct, and often consist of semiconductor electrode and an auxiliary electrode immersed in an electrolyte containing adequate redox couple and exposed to sunlight. The auxiliary electrode is responsible for the regeneration of the redox species and generally covered with metals to catalyze this reaction. The counter electrode used in this study is ITO-glass coated with oxidized poly(3,4-ethylenedioxythiophene), PEDOT. PEDOT is required on ITO because it improves the charge transfer between ITO and the iodide/triiodide redox couple. It is known that bare ITO is irreversible for the iodide/triiodide oxidation/reduction reaction [63]. A common layout of the PEC solar cells is shown in Fig. 2.8. In the photoelectrochemical solar cell a semiconductor-electrolyte junction is used as a photoactive layer. The semiconductor is responsible for the absorption

of the incident light, while the interface between the semiconductor and the electrolyte is the key factor in the subsequent chemical steps that lead to energy conversion.

An illuminated PEC bears a formal resemblance to a traditional Schottky barrier photovoltaic device, with the metal layer connecting the semiconductor replaced by an electrolyte containing an adequate redox couple. In contrast to the all-solid conventional semiconductor solar cells, PEC solar cell uses a liquid electrolyte or ion-conducting solid phase as a charge transport medium. For commercial applications the use of liquid electrolytes, such as the I_3^-/I^- redox couple dissolved in acetonitrile, limits the application of photoelectrochemical cells.

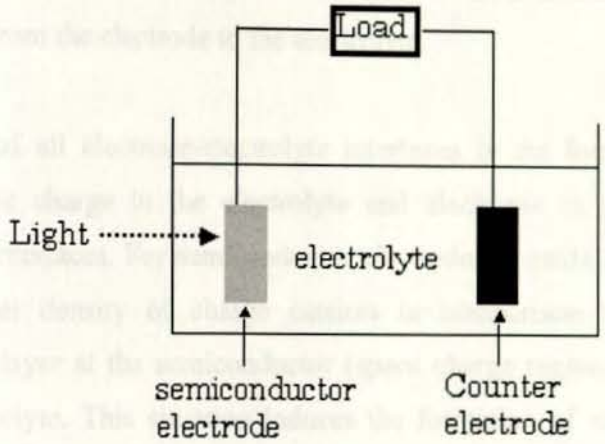

Fig. 2.8. The common layout of photoelectrochemical solar cell.

Inorganic semiconductors are the natural candidates for use in photoelectrochemical cells. The most promising candidates to replace the inorganic semiconductors in the assembly of solar cells are organic materials, due to their photosensitivity and photovoltaic effects. The most well-known and studied unconventional photovoltaic system is the dye sanitized nano-structured solar cell developed by Gratzel in 1991 [64]. At the moment this unique photoelectrochemical solar cell based on a TiO_2 nanoparticle photoelectrode with light harvesting metallic-organic dye, is on the verge of commercialization offering an interesting alternative for the existing silicon based solar cells as well as for the thin film solar cells. At

the same time the research activity as well as the industrial interest around the technology is growing fast.

In the following section the basic principles of photoelectrochemical solar energy will be discussed.

2.6.2. The Semiconductor/Electrolyte Interface

When a semiconductor electrode is in contact with an electrolytic solution, a charge transfer occurs through the interface providing equilibrium between the Fermi level of the semiconductor and the redox potential of the solution. Considering a *p*-type semiconductor immersed in an electrolyte with redox potential higher than the semiconductor Fermi level, an electron transfer from the electrode to the electrolyte.

A common aspect of all electrode-electrolyte interfaces is the formation of electrically charged layers (ionic charge in the electrolyte and electronic in the electrode) with a capacitance related interfaces. For semiconductor electrodes a special situation is that these materials have lower density of charge carriers in comparison to metals. Thus, the electrically charged layer at the semiconductor (space charge region) is broader than that formed in the electrolyte. This situation induces the formation of an electric field in the space charge region, leveling the semiconductor Fermi level and the redox potential of the electrolyte solution, producing a band bending close to the electrolyte boundary, as shown in Fig. 2.9 for a p-type semiconductor. This electric field is responsible for electron and holes transport at the interface. At the surface, the semiconductor becomes depleted of majority carriers (for a *p*-type semiconductor, holes) and a depletion layer is formed.

Irradiating the semiconductor with incident light intensity greater than the band gap energy, valence band electrons are promoted to the conduction band, forming an electron-hole pair, also called exciton. In *p*-type semiconductors, it causes the migration of minority carriers (electrons) towards the interface, while majority carriers (holes) diffuse to the semiconductor bulk. At the boundary, the electrons, being regenerated at the counter

electrode, producing the photocurrent in a short-circuited system, reduce the oxidized species in the electrolyte solution. For *n*-type semiconductors the majority carriers are the electrons and the inverse behavior occurs. Additionally, the potential where no excess of charge exists is called zero charge potential and, under these conditions, the space charge region disappears and the bands do not bend. The potential where this situation occurs is known as flat band potential. These processes are the basic operation mode of regenerative photoelectrochemical cells.

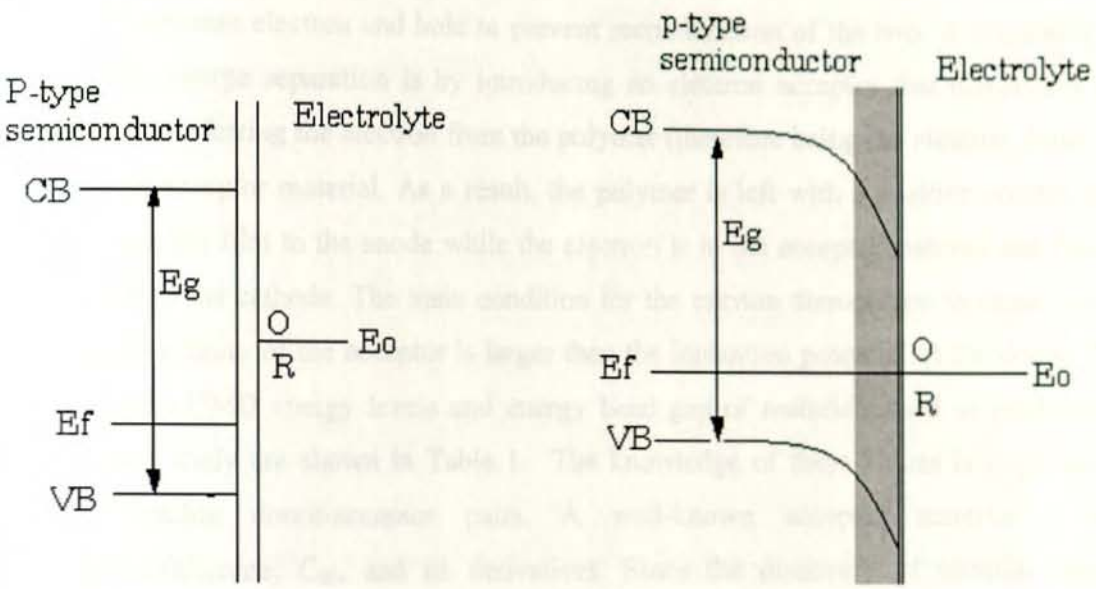

a) b)

Fig. 2.9. Representation of the formation of the Schottky junction between a p-type semiconductor and an electrolyte containing a redox couple O/R: a) before the contact, b) after the contact, considering the redox potential of the electrolyte is higher than the semiconductor Fermi level.

2.7. Conjugated Polymer-Fullerene Heterojunction Solar Cells

For solar cells made with pure conjugated polymers, energy conversion efficiency is too low to be used in practical applications. Thus photoinduced charge transfer across a

donor/acceptor interface provides an effective method to overcome early time carrier recombination in organic systems and thus to enhance their optoelectronic response.

In most conjugated polymers, the predominant excited species is the singlet exciton. At room temperature the electron and hole are bound to each other and there are no free charge carriers. An essential process for polymeric solar cells after photoexcitation is charge separation. Since the electron and hole are bound together, a mechanism must be found to efficiently separate electron and hole to prevent recombination of the two. A possibility to achieve this charge separation is by introducing an electron acceptor that dissociates the exciton by transferring the electron from the polymer (therefore being the electron donor) to the electron acceptor material. As a result, the polymer is left with a positive polaron that drift through the film to the anode while the electron is in the acceptor material and can be transported to the cathode. The main condition for the exciton dissociation to occur is that the electron affinity of the acceptor is larger than the ionization potential of the donor. The HOMO and LUMO energy levels and energy band gap of materials used as photoactive layer in this study are shown in Table 1. The knowledge of these values is required for finding suitable donor-acceptor pairs. A well-known acceptor material is the Buckminsterfullerene, C_{60}, and its derivatives. Since the discovery of ultrafast charge transfer from conjugated polymers to C_{60} by Sariciftci *et al* [59], its properties as an electron acceptor have been subject of intense research. The charge transfer typically occurs within the femtosecond time regime. An upper limit was found to be 300 fs [65], which is three orders of magnitude faster than an electron-hole recombination process within the polymer.

There are two general ways to create a donor-acceptor interface in organic devices. One is to bring two films in contact at the surface, which creates a heterojunction. In this case, only a fraction of the bulk of the material builds a donor-acceptor interface. The other is to blend the two materials to form one mixed layer. In this case, the whole bulk of the device has a donor-acceptor interface. These devices are called bulk-heterojunction devices. Early studies showed the importance of close proximity of polymer and fullerene for the efficiency of photovoltaic devices.

Formation of bulk heterojunction by mixing the polymer (donor) and the fullerene (acceptor) lead to an enhancement of short circuit current density due to an increased interface area for charge separation. However, it is still much lower than the short circuit current density reported for inorganic devices. This lower photocurrent is due to the limited transport of the separated charge carriers to the electrodes due to the low charge carrier mobility in organic materials. On the other hand, organic solar cells produce quite respectable open-circuit voltages.

Table 1. The HOMO and LUMO energy levels and energy gap of P3HT [66], MDMO-PPV [67] and C_{60} [68].

Material	HOMO level (eV)	LUMO level (eV)	Band gap (eV)
P3HT	-5.40	-3.20	2.20
MDMO-PPV	-5.30	-2.83	2.47
C_{60}	-6.10	-3.70	2.40

Organic photovoltaic cells with blends of conjugated polymers and fullerenes as a photoelectrode was extensively studied; and maximum power conversion efficiencies up to 2.5 % under AM1.5 illumination have been reported [17]. But there is no report on donor-acceptor composite photoelectrode based solid-state photoelectrochemical cells. In this work the all-solid-state PEC cell with blends of conjugated semiconducting polymers and fullerene is developed for the first time and its solar cell behavior is studied.

2.8. Solar Cell Parameters

In solar cells the photon energy is converted into electrical energy. When a sheet of solar cell material is exposed to sunlight, a photon with energy greater than or equal to the band gap energy, E_g, of the semiconductor is absorbed in the cell thereby generating photocurrent. On the other hand, photon energy less than E_g makes no contribution to the cell out put. The incident photon energy depends on the wavelength of the light and hence the band gap energy, E_g, is related to the wavelength.

To derive the solar cell output parameters that are used for characterization of photoelectrochemical properties of the device, we shall consider an ideal Schottky diode. When the cell is illuminated, the total current density, I, is equal to the sum of the photocurrent density, I_{ph}, and the dark current density, I_{dark}.

$$I = I_{ph} - I_{dark} \tag{1}$$

The dark current-voltage characteristics of the solar cell is expressed as

$$I = I_0\left[\exp\left(\frac{qV}{nkT}\right)-1\right] \tag{2}$$

where I is the total current density (dark current density), I_0 is the inverse saturation current density which is the current density flowing under sufficiently high reverse bias, q is the charge on an electron, V is the applied voltage, n is the ideality factor of the diode (for an ideal diode n = 1), k is the Bolzmann constant and T is the absolute temperature.

Thus the I-V characteristics of the Schottky diodes under illumination is given by

$$I = I_{ph} - I_0\left[\exp\left(\frac{qV}{nkT}\right)-1\right] \tag{3}$$

The ideal I-V characteristics of the solar cell under illumination is shown in Fig. 2.10.

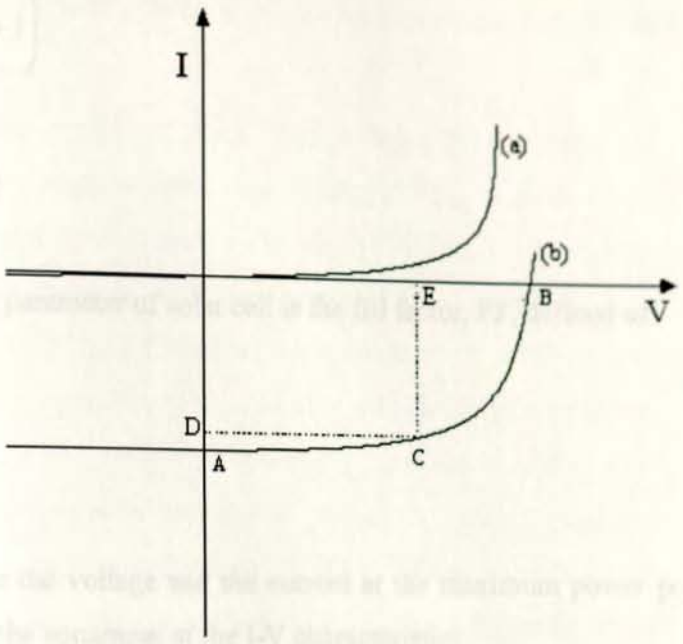

Fig. 2.10. Typical current density-voltage characteristics of Schottky diodes (a) in the dark (b) under illumination. A) I_{sc}, B) V_{oc}, C) P_{max}, D) I_{mp}, E) V_{mp}.

The three parameters that are used to characterize the photovoltaic properties of the cell are derived from the I-V characteristics Eqn. (3) of the Schottky diode.

Short-circuit current

The short-circuit current *(I_{sc})* corresponds to point A, in Fig. 2.10. It is the condition where photocurrent flows under zero applied voltage. It is obtained by substituting V = 0 into Eqn. (3). Ideally it is equal to the current density, I_{ph}, generated by light.

$$I_{sc} = I_{ph} \tag{4}$$

Open-circuit voltage

The open circuit voltage *(V_{oc})* is obtained by setting I = 0 into Eqn. (3). This is the condition where photovolatge is generated but no photocurrent flows (point B in Fig. 2.10)

$$V_{oc} = \frac{nkT}{q} \ln\left(\frac{I_{ph}}{I_0} + 1\right) \tag{5}$$

Fill-factor (FF)

Another important parameter of solar cell is the fill factor, FF, defined as

$$FF = \frac{V_{mp} I_{mp}}{V_{oc} I_{sc}} \tag{6}$$

where V_{mp}, I_{mp} are the voltage and the current at the maximum power point (point C Fig. 2.10). It measures the squarness of the I-V characteristics.

Power conversion Efficiency

The energy conversion efficiency of the solar cell in converting light energy into useful electrical energy is the most important quantity defining the quality of the cell. In the I-V curve of the Schottky diode (Fig. 2.10) point C corresponds to the maximum power point, where the product of photovolatge, $V_{mp,}$ and photocurrent,I_{mp}, is maximum. The energy conversion efficieny, η, is then given by

$$\eta = \frac{V_{mp} I_{mp}}{P_{in}} = \frac{V_{oc} I_{sc} FF}{P_{in}} \tag{7}$$

where P_{in} is the intensity of the light incident on the cell.

Incident monochromatic photon to current conversion efficiency (IPCE)

One of the most important parameters when studying the performance of solar cells is the incident photon to current conversion efficiency, IPCE. It is defined as the ratio of the number of collected charge carriers to the number of incident photons at the device. As the name suggests, the value is commonly measured for a specific light wavelength. One advantage of analyzing the IPCE rather than photocurrent is that effects due to the spectral shape of the incident light, due to light source or measurement equipment, are removed and the true response of the device is obtained. Understanding the reasons for obtaining a specific IPCE of a device is essential to obtain fundamental understanding and thus to improve the device performance. Plots of IPCE versus wavelength illustrate the spectral operation range of a specific solar cell. For high performance solar cells, the IPCE value can reach unity over a large spectral section. The IPCE were calculated as the ratio of the observed photocurrent density and the photon density incident on the cell:

$$IPCE\% = \frac{1240 I_{sc}}{\lambda P_{in}} \tag{8}$$

where I_{sc} is short circuit current ($\mu A\ cm^{-2}$), λ the excitation wavelength (nm) and P_{in} the incident photon intensity (Wm^{-2}). Light of different wavelength is absorbed at different depths of the photoactive electrode.

3. EXPERIMENTAL

3.1. Materials

In this study the conjugated semiconducting polymers used as photoactive electrodes are poly(3-hexylthiophene) (P3HT) (Aldrich) & poly(2-methoxy-5-(3',7'-dimethyloctyoxyl)-1,4- phenylenevinylene) (MDMO-PPV) (Aldrich). Buckminsterfullerene,C_{60}, is used as an electron acceptor molecule. The polymer electrolyte used is amorphous poly(ethylene oxide), POMOE, with a repeating unit of $CH_2O(CH_2CH_2O)_9$. The redox couple used to complex with the polymer is iodine/triiodide. The counter electrolyte used is ITO-glass coated with oxidized poly(3,4-ethylenedioxythiophene), PEDOT. The chemical structures of the conjugated polymers and the acceptor molecule used in this work are depicted in Fig. 3.1.

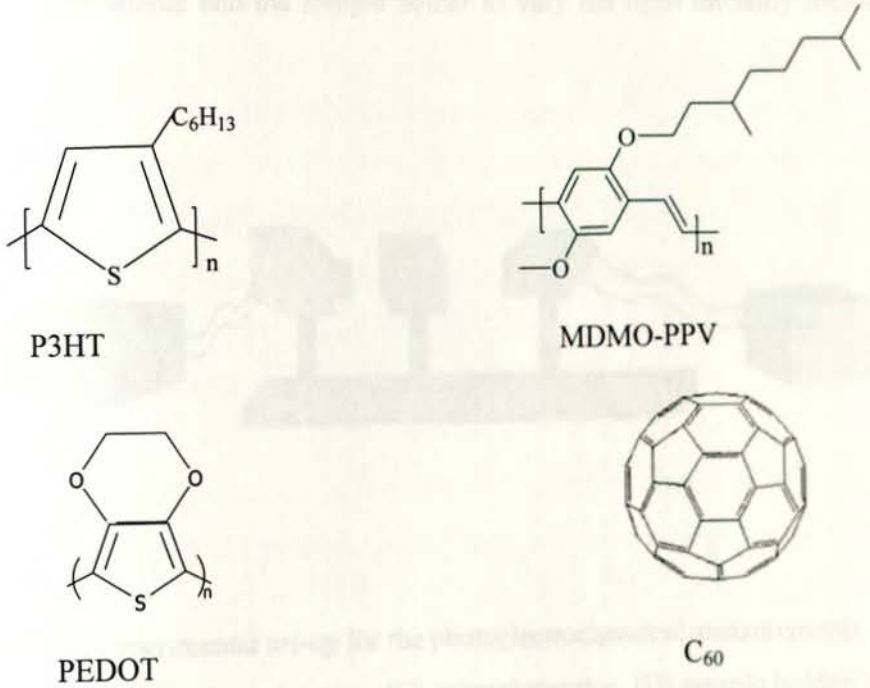

Fig. 3.1. The chemical structure of conjugated polymers used in this work and the acceptor molecule, Buckminsterfullerene, C_{60}.

3.2. Experimental Set-up

A schematic of the experimental set-up used to measure the photoelectrochemical properties of the device is shown in Fig. 3.2. A 250 W tungsten-halogen lamp regulated by an Oriel power supply (Model 66182) is used to illuminate the PEC. A grating monochromator (Model 77250) is used to select a wavelength between 300 and 800 nm. The resulting photoelectrochemical properties were studied using CHI600A Electrochemical Analyzer. All spectra were corrected for the spectral response of the lamp and the monochromator by normaliztion to the response of a calibrated silicon photodiode (Hamamatsu, model S-1336-8BK). The white light intensity was measured in the position of the sample cell with a Conrad electronic luxmeter (Model LX-101).

For intensity dependence measurements a series of neutral density filters were placed between the light source and the sample holder to vary the light intensity incident on the sample.

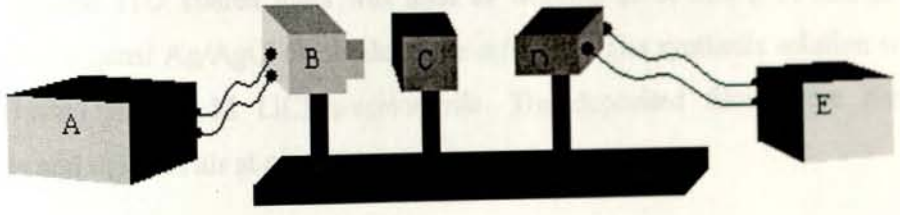

Fig. 3.2. General experimental set-up for the photoelectrochemical measurements. (A) power supply, (B) lamp housing, (C) monochromator, (D) sample holder, and (E) an output measuring apparatus.

3.3. Sample Preparation and Device Structure

The device is fabricated on indium tin oxide (ITO) coated glass substrate. The ITO coated glass is cut to a 2.5 cm x 1.5 cm square and cleaned successively with distilled water, acetone and ethanol and dried with an air gun. For optical absorption measurement the conjugated polymers mixed with Fullerene were dissolved in o-dichlorobenzene and solvent (drop) cast on the ITO-glass. The optical absorption spectrum of the films was measured using Spectroscopic GENESYS 2PC UV-Vis spectrometer.

The photoactive layer was prepared by mixing 5 mg conjugated semiconducting polymer with 5 mg Fullerene. This mixture was then dissolved in 1 mL o-dichlorobenzene solution. A solution of 5 mg pure MDMO-PPV in 1 mL of dichlorobenzene was also prepared. Photoactive electrodes were formed by drop casting solutions of P3HT/C_{60}, MDMO-PPV/C_{60} and MDMO-PPV separately on pre-cleaned ITO coated glass substrates.

For counter electrode, films of PEDOT were potentiostatically deposited on a pre-cleaned ITO-coated glass at a potential of 2 V for 4 seconds in a single compartment three-electrode cell. Pre-cleaned ITO coated glass was used as working electrode; a Pt foil as counter-electrode and a quasi Ag/AgCl electrode as the reference. The synthesis solution was 0.1 M EDOT (Bayer) in 0.1 M $LiClO_4$-acetonitrile. The deposited films were rinsed with acetonitrile and dried in air at room temperature.

Quasi Ag/AgCl reference electrode (silver wire coated with silver chloride) was prepared by applying 4.6 V to silver and platinum wires immersed in a saturated potassium chloride solution.

The polymer electrolyte was prepared by dissolving 312.5 mg of POMOE in 25 ml of methanol. The redox couple I_3^- / I^- was prepared by dissolving 49 mg KI and 7.4 mg I_2 in 25 ml of methanol separately. Finally, 2 mL of each solution was mixed to produce the polymer electrolyte complexed with a redox couple. The mole ratio of oxygen to potassium as calculated by taking into account both the oxymethylene and oxyethylene oxygen atoms was

25 and the mole ratio of KI to I_2 was 10, i.e., the concentration of I_2 is one tenth the concentration of KI. The conductivity of POMOE is known to be high at room temperature when the oxygen to cation mole ratio is 25 [68].

Finally, the polymeric electrolyte solution was drop casted on the photoactive layer coated ITO- glass, allowed to dry, and pressed against PEDOT coated ITO-glass counter electrode. Then, the devices were mounted in a sample holder with 1 cm^2 opening to allow light from the source.

The general device structure of all-solid state PECs used in this work is shown in Fig. 3.3. The device consisting of electrically conducting conjugated polymer mixed with fullerene, ionically conducting solid polymer electrolyte complexed with redox couple and a PEDOT coated on ITO counter electrode. Illumination of the device was done through the ITO/photoactive layer (back side) or the PEDOT/ITO (front side).

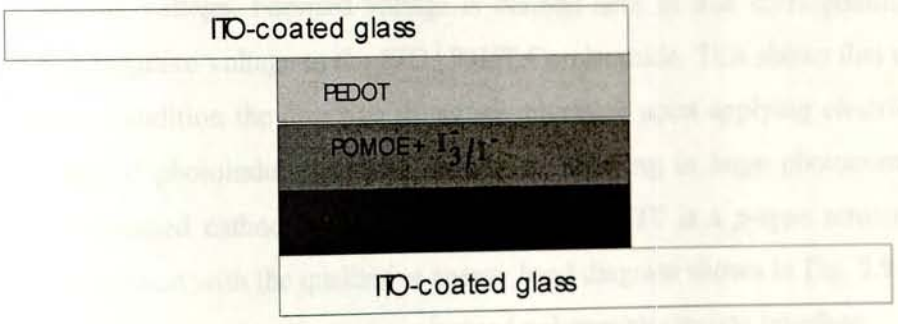

Fig. 3.3. The basic structure of solid-state PEC used in this work

4. RESULTS AND DISCUSSION

4.1. Solid state photoelectrochemical solar energy conversion based on blend of P3HT and C_{60}

4.1.1. Current – Voltage characteristics

The current density-voltage characteristic in the dark, as well as under illumination was measured. The current density-voltage characteristics of ITO | P3HT:C_{60} | POMOE:I_3^-/I^- | PEDOT | ITO solid-state PEC in the dark and under illumination are shown in Fig. 4.1.1. The device was illuminated through PEDOT | ITO side. The effective area of the solar cell was 1 cm^2. The intensity of the white light incident on the cell was approximately 100 $mWcm^{-2}$. The device exhibits a rectification character in the dark. The rectifying property of the device in the dark indicates that ITO | P3HT:C_{60} | POMOE:I_3^-/I^- | PEDOT | ITO cell has desirable photoelectrochemical property. Under illumination, the ITO | P3HT:C_{60} | POMOE:I_3^-/I^- | PEDOT | ITO cell exhibits cathodic photocurrent under zero applied voltage. As it can be seen from the I-V curve the cathodic photocurrent increases with increasing forward voltage. Forward voltage is defined here as that corresponding to the application of a negative voltage to the ITO | P3HT:C_{60} electrode. This shows that under the negative voltage condition the direction of carrier migration upon applying electric field is the same as that of photoinduced charge separation, resulting in large photocurrent. This generation of increased cathodic photocurrent indicates P3HT is a *p*-type semiconductor. This result is consistent with the qualitative energy band diagram shown in Fig. 2.9 that may be formed at the *p*-type semiconducting conjugated polymer/electrolyte interface.

To compare the photoelectrochemical properties under the same illumination condition for solid-state PEC cells based on the pure P3HT and P3HT:C_{60} composite photoactive electrodes, the typical photoelectrochemical parameters have been calculated from the analysis of their I-V characteristics and listed in Table 2. The short-circuit current density and open circuit voltage of the devices are I_{sc} = 0.47 $\mu A/cm^2$ and V_{oc} = 130 mV for P3HT [14]; and I_{sc} = 7.28 $\mu A/cm^2$ and V_{oc} = 97.8 mV for P3HT:C_{60} composite electrode cell.

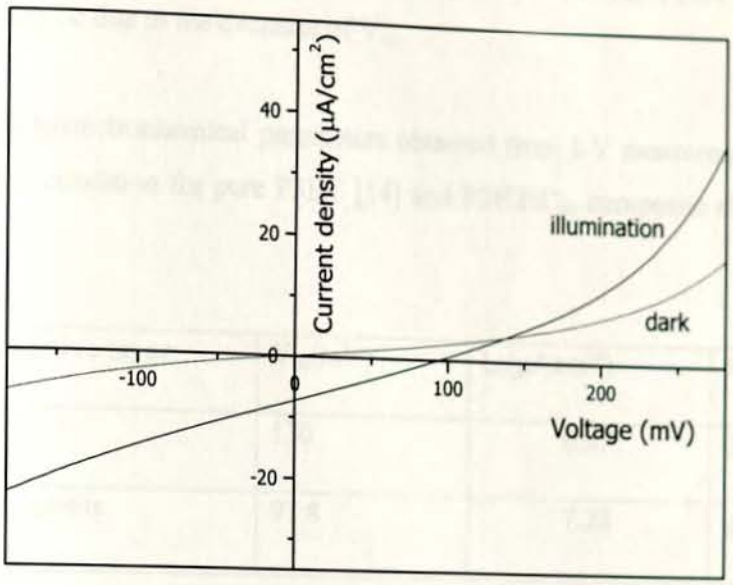

1.1. Current density-voltage characteristics of ITO | P3HT:C_{60} | POMOE:I_3^-/I^- OT | ITO cell in the dark and under illumination through front side with light ty of 100 mWcm^{-2} at a scan rate of 1 mV/s.

sult shows that the P3HT:C_{60} composite based PEC has lower V_{oc} but greater I_{sc} than that of the pure PEC, as it is the case for other types of organic photovoltaic cells ends of p-type conjugated polymer and fullerene [69]. The reason for the decrease in ıen C_{60} is incorporated into the photoactive electrode is not yet clear. However, it is ed that in two component charge transfer systems deviations of the V_{oc} from the of pure conjugated polymer devices may be because of some part of the available ıce in electrochemical energy is used internally by the charge transfer to a lower ic position on the electron acceptor. Hence, decrease of V_{oc} is probably associated ınning of P3HT Fermi level to the reduction potential of C_{60}. The incorporation of ı acceptors into p-type conjugated polymers in photoactive electrode always es photocurrent of the device due to the ultra fast photoinduced electron transfer from ated polymers to acceptor molecules [5]. Hence, the large increase in the photocurrent

for P3HT:C_{60} composite electrode PEC could be result of the ultrafast photoinduced electron transfer from P3HT to C_{60} molecule. The slightly lower FF for P3HT:C_{60} composite electrode PEC may be due to the decrease of V_{oc}.

Table 2. The photoelectrochemical parameters obtained from I-V measurements under the same illumination condition for pure P3HT [14] and P3HT:C_{60} composite electrodes based solid state PECs.

Photoactive layer	V_{oc}(mV)	I_{sc}(μAcm^{-2})	FF
Pure P3HT	130	0.47	0.31
P3HT:C_{60} composite	97.8	7.28	0.26

4. 1. 2. Time dependence of I_{sc} and V_{oc}

The time dependence of short-circuit current density and open circuit voltage were measured. These measurements were used to characterize the stability of the cell towards illumination.

Figures 4.1.2 and 4.1.3, respectively, show the short-circuit current and open circuit voltage as a function of time for ITO | P3HT:C_{60} | POMOE:I_3^-/I^- | PEDOT | ITO solid-state PEC. The illumination was made from the PEDOT | ITO (front side) with a white light intensity of 100 $mWcm^{-2}$. The generation of photovoltage and photocurrent were rapid and reproducible under several on-off cycles of illumination. The stability of both the photocurrent and photovoltage were very good. The steady state values of short circuit photocurrent density and open-circuit photovoltage were 7.5 $\mu A/cm^2$ and 98.5 mV, respectively.

The results of time dependence study show that the steady state I_{sc} and V_{oc} values are consistent with those obtained in the I-V curve.

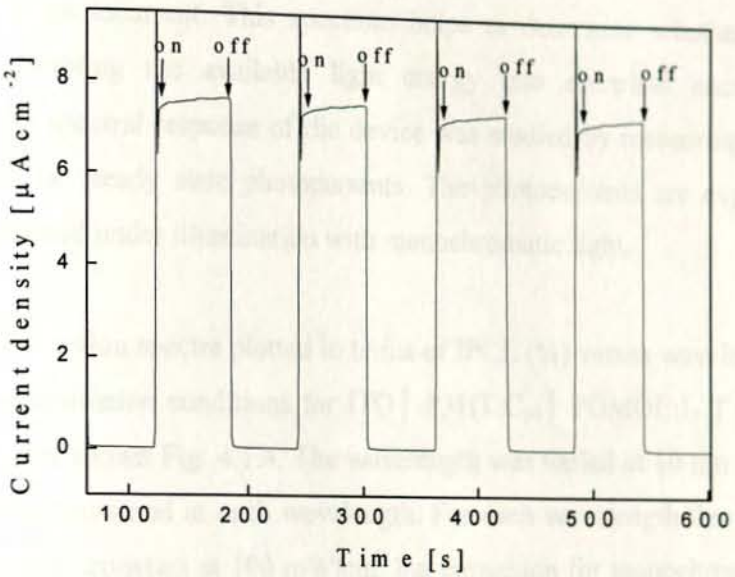

Fig. 4.1.2. Photocurrent response to switching illumination on and off from the front side of ITO | P3HT:C_{60} | POMOE:I_3^-/I^- | PEDOT | ITO solid-state PEC.

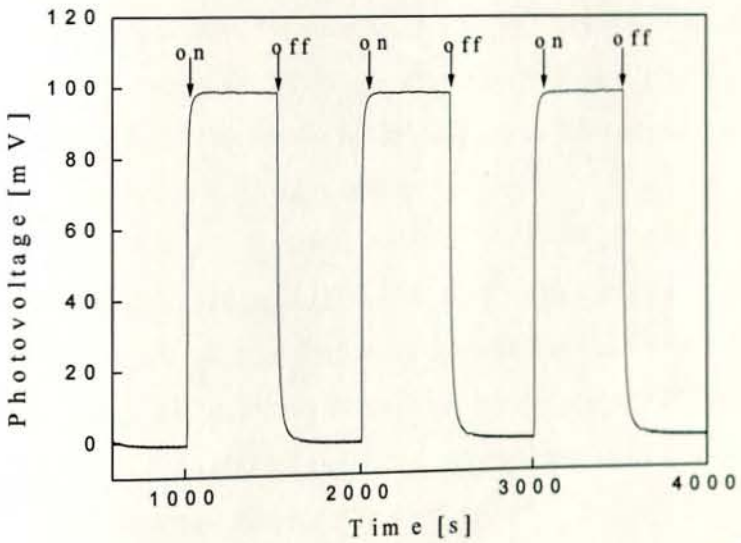

Fig. 4.1.3. Photovoltage response to switching illumination on and off from the front side of ITO | P3HT:C_{60} | POMOE:I_3^-/I^- | PEDOT | ITO solid state PEC.

4. 1. 3. Spectral responses

Another important property of a solar cell is the spectral response for which it absorbs light and produces a photocurrent. This spectrum helps to determine whether a solar cell is capable of converting the available light energy into electrical energy at different wavelength. The spectral response of the device was studied by measuring the wavelength dependence of the steady state photocurrents. The photocurrents are expressed as IPCE which were obtained under illumination with monochromatic light.

The photocurrent action spectra plotted in terms of IPCE (%) versus wavelength under front and backside illumination conditions for ITO | P3HT:C_{60} | POMOE:I_3^-/I^- | PEDOT | ITO solid-state PEC is shown Fig. 4.1.4. The wavelength was varied at 10 nm intervals and the photocurrent was measured at each wavelength. For each wavelength the light intensity of the source was kept constant at 100 mW/cm^2 but correction for monochromatic intensity at the different wavelength was made when calculating the IPCE. The maximum value of the IPCE is found to be 0.43 % for front side illumination and 0.01% for backside illumination at a wavelength of 510 nm.

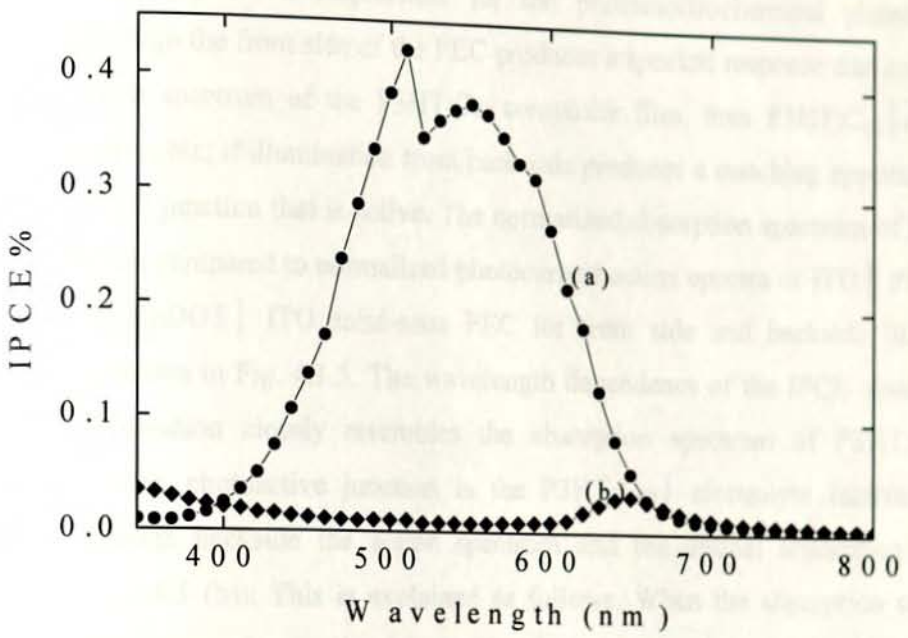

Fig. 4.1.4. Photocurrent action spectra for ITO | P3HT:C_{60} | POMOE:I_3^-/I^- | PEDOT | ITO solid-state PEC illuminated through (a) front side and (b) backside.

Comparison of front side and backside conversion efficiencies showed that front side illumination is greater than backside illumination at the maximum absorbance. The reason behind this difference lies on the optical filtering effect of the P3HT:C_{60} composite film. When light is illuminated from the backside, only small fraction of the excitons (bound electron-hole pairs) produced by light absorption reach the interface to dissociate into carriers. Moreover, the presence of a high density of the traps in the film reduces the number of carriers for the photocurrent generation. The greater the distance from the surface, the smaller is the probability for an exciton to reach the interface and dissociate into carriers.

The IPCE (%) values at the maximum absorbance for the pure P3HT based PEC is 0.024 from front side and 0.003 from back side illumination conditions [14]. The high values of IPCE for P3HT:C_{60} composite electrode based PEC is due to greater photocurrent of the cell.

Comparison of the optical absorption spectrum and spectral photoresponse can be used to identify the active junction responsible for the photoelectrochemical phenomena. If illumination through the front side of the PEC produces a spectral response that corresponds to the absorption spectrum of the P3HT:C_{60} composite film, then P3HT:C_{60} | electrolyte junction is responsible; if illumination from back side produces a matching spectrum, then it is P3HT:C_{60} | ITO junction that is active. The normalized absorption spectrum of P3HT:C_{60} composite film as compared to normalized photocurrent action spectra of ITO | P3HT:C_{60} | POMOE:I_3^-/I^- | PEDOT | ITO solid-state PEC for front side and backside illumination conditions are shown in Fig. 4.1.5. The wavelength dependence of the IPCE obtained from front side illumination closely resembles the absorption spectrum of P3HT:C_{60} film, indicating that the photoactive junction is the P3HT:C_{60} | electrolyte interface. When illuminated through backside the action spectrum and the optical absorption spectrum mismatch (Fig. 4.1.5 (b)). This is explained as follows. When the absorption constant is high, excitons are created very close to the ITO | photoactive layer (backside). Therefore, only a small fraction of the light reaches the barrier regions when illuminated through the back contact and as a result charge carriers are lost due to recombination or trapping which decreases the photocurrent. However at wavelengths where the absorption constant is low, light penetrates deeper and the excitons will be created much closer to the photoactive electrode/polymer electrolyte interface so that a relatively large photocurrent will be measured. Only charge carriers in or near the space charge region of the active junction have a significant probability of being collected for the external circuit. Thus photons absorbed away from the active junction generally have no effect on photocurrent generation.

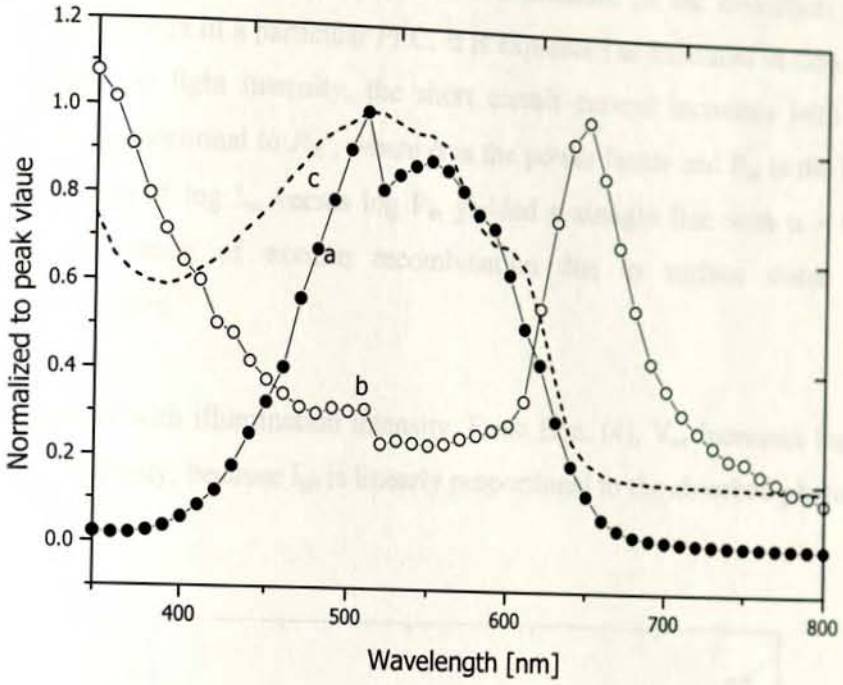

Fig. 4.1.5. Photocurrent action spectrum of ITO/P3HT:C_{60}/I^-:I_3^-/PEDOT/ITO for illumination through a) front side b) back side; and c) optical absorption spectrum of P3HT:C_{60} blend deposited on ITO normalized to the peak value.

4.1.4. I_{sc} and V_{oc} dependence on incident light intensity

The short-circuit current density and open circuit voltage dependence of the solid-state PEC on the incident light intensity were studied. For intensity dependence measurements, the experimental set-up was modified in such a way that a neutral density optical filter was placed between the light source and the sample. The fate of the photogenerated electrons and holes is crucial for the device efficiency; therefore, the influence of light intensity on the I_{sc} and V_{oc} is important.

The plot of log I_{sc} and V_{oc} versus the log P_{in} of ITO | P3HT:C_{60} | POMOE:I_3^-/I^- | PEDOT | ITO solid-state PEC is shown in Fig. 4.1.6 and 4.1.7, respectively. The illumination intensity was varied from 0.01 to 100 $mWcm^{-2}$. To rationalize the dependence of I_{sc} and V_{oc} on

incident light intensity we should take into account the expressions used to define these parameters in *p-n* junction diode. I_{sc} provides a measure of the collection efficiency of photogenerated carriers in a particular PEC. It is expressed as indicated in Eqn.(4). Since I_{ph} depends linearly on light intensity, the short circuit current increases with illumination intensity and is proportional to P_{in}^{α}, where α is the power factor and P_{in} is the incident light intensity. The plot of log I_{sc} versus log P_{in} yielded a straight line with $\alpha = 0.91$. $\alpha < 1$ indicates the presence of exciton recombination due to surface states that act as recombination centers.

V_{oc} also increases with illumination intensity. From Eqn. (4), V_{oc} increases logarithmically with the light intensity, because I_{ph} is linearly proportional to the absorbed photon intensity.

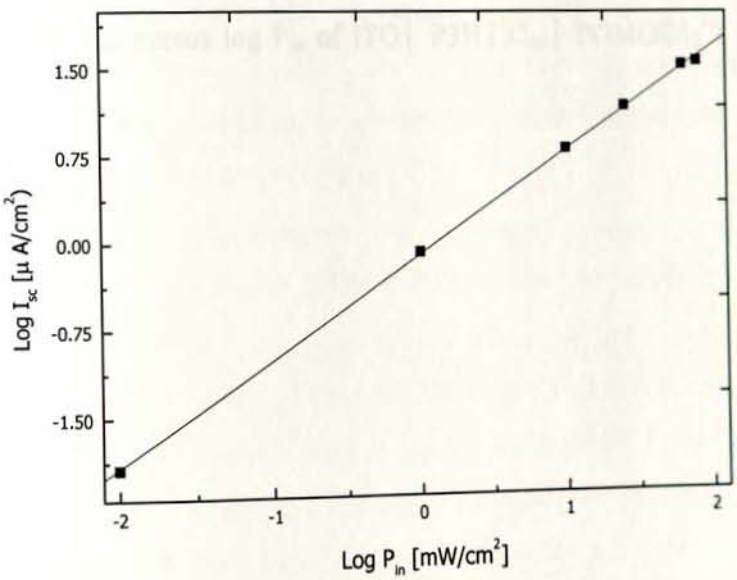

Fig. 4.1.6. Plot of log I_{sc} versus log P_{in} of ITO | P3HT:C_{60} | POMOE:I_3^-/I^- | PEDOT | ITO solid-state PEC.

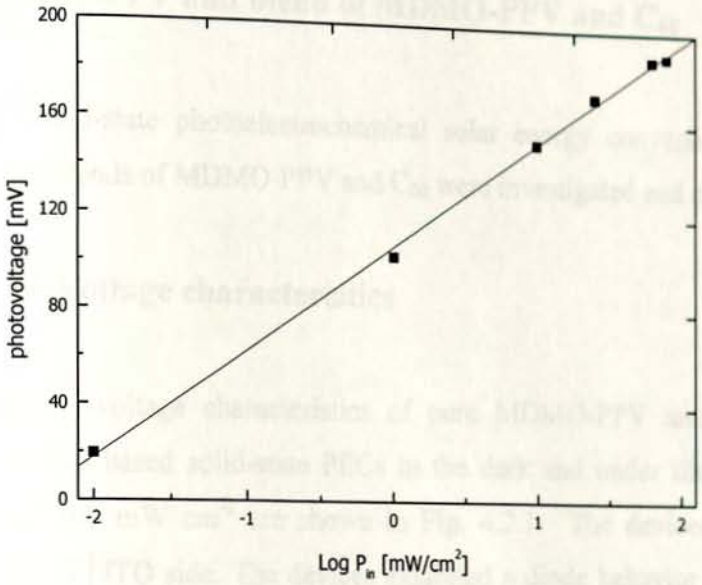

Fig. 4.1.7. Plot of V_{oc} versus log P_{in} of ITO | P3HT:C_{60} | POMOE:I_3^-/I^- | PEDOT | ITO solid-state PEC.

4.2. Solid state photoelectrochemical solar energy conversion based on pure MDMO-PPV and blend of MDMO-PPV and C_{60}

In this section solid-state photoelectrochemical solar energy conversion based on pure MDMO-PPV and blends of MDMO-PPV and C_{60} were investigated and compared.

4.2.1. Current-Voltage characteristics

The current density-voltage characteristics of pure MDMO-PPV and MDMO-PPV:C_{60} composite electrodes based solid-state PECs in the dark and under illumination with the light intensity of 100 mW cm^{-2} are shown in Fig. 4.2.1. The devices were illuminated through the PEDOT | ITO side. The devices exhibited a diode behavior in the dark, which indicates that the cells have desirable photoelectrochemical property. The current at the negative potential range remains relatively low while at positive potential a larger current is noticed. Under illumination a much larger cathodic current is observed when a negative voltage is applied on ITO | MDMO-PPV and ITO | MDMO-PPV:C_{60} composite electrodes. The increase in cathodic photocurrent with increasing potential towards the negative direction indicates that the neutral MDMO-PPV is a p-type semiconductor. This result suggests that under negative applied voltage condition the direction of carrier migration upon applying electric field is the same as that of photoinduced charge separation, resulting in large photocurrent. The incorporation of C_{60} into MDMO-PPV caused no effect on I-V characteristics of the PECs in the dark but resulted in significant change in the I-V character under illumination of the PEC, as it is the case for other types of organic photovoltaic devices with blends of conjugated semiconducting polymer and fullerene photoactive electrodes.

The photoelectrochemical parameters obtained from the I-V characteristics of MDMO-PPV:C_{60} composite based solid-state PEC as compared to that of the pure MDMO-PPV are shown in Table 3.

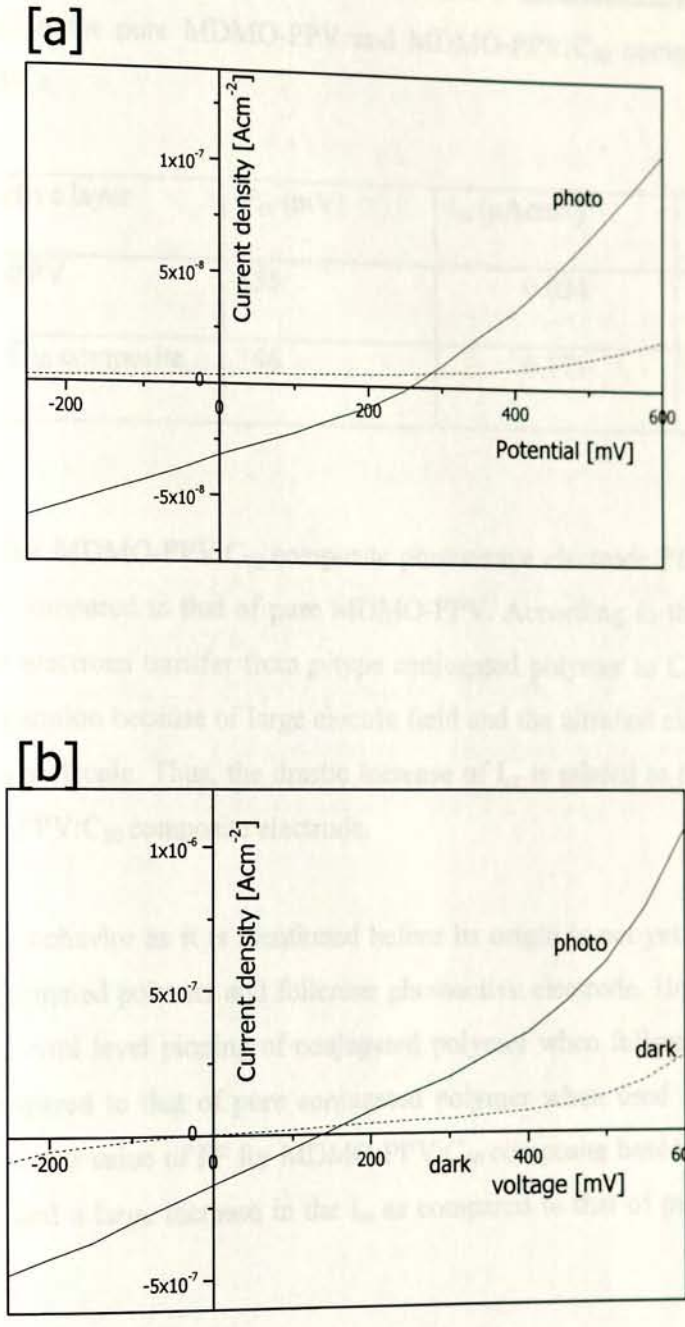

Fig. 4.2.1. Current-Voltage characteristics the all-solid-state PEC in the dark (-----) & under white light illumination (——) for **[a]** pure MDMO-PPV and **[b]** blend of MDMO-PPV/C_{60}

Table 3. Photoelectrochemical parameters obtained from I-V measurements under the same illumination condition for pure MDMO-PPV and MDMO-PPV:C_{60} composite electrodes based solid state PECs.

Photoactive layer	V_{oc} (mV)	I_{sc} (μAcm^{-2})	FF
Pure MDMO-PPV	255	0.034	0.28
MDMO-PPV:C_{60} composite	146	0.171	0.25

The results show that MDMO-PPV:C_{60} composite photoactive electrode PEC has larger I_{sc} and smaller V_{oc} as compared to that of pure MDMO-PPV. According to the literature [70] the photogenerated electrons transfer from *p*-type conjugated polymer to C_{60} underwent an efficient charge-separation because of large electric field and the ultrafast electron accepting property of the C_{60} molecule. Thus, the drastic increase of I_{sc} is related to the better charge transfer in MDMO-PPV:C_{60} composite electrode.

Concerning the V_{oc} behavior as it is mentioned before its origin is not yet clear in organic solar cells with conjugated polymer and fullerene photoactive electrode. However, it can be estimated that the Fermi level pinning of conjugated polymer when fullerene is added will reduce the V_{oc} compared to that of pure conjugated polymer when used as a photoactive electrode. Slightly lower value of FF for MDMO-PPV:C_{60} composite based cell may be due to decrease of V_{oc} and a large increase in the I_{sc} as compared to that of pure MDMO-PPV PEC.

4.2.2. Time dependence of I_{sc} and V_{oc}

To see the stability of the photoactive electrode towards irradiation and to evaluate the steady state photocurrent and photovoltage in the absence of any external applied electric field, the photocurrent-time and photovoltage-time characteristics were examined for the

PECs with illumination through the front side at the incident light intensity of approximately 100 $mWcm^{-2}$. Fig. 4.2.2 and Fig. 4.2.3 show the time-dependent response of the short-circuit current and the open circuit voltage, respectively, of the two solid-state PECs. In both cases a very low current is observed before the onset of light (Fig. 4.2.2). When switching the illumination on, the current increases steadily and stays fairly constant during the remaining illumination time. When the light was turned off most of the photocurrent decayed abruptly. The systems were more or less stable to irradiation, where no significant decay was noticed for a longer time of illumination. The steady state photocurrents observed by switching the illumination on are 0.03 and 0.23 $\mu A/cm^2$ for ITO | MDMO-PPV | I^-:I^-_3 | PEDOT | ITO&ITO | MDMO-PPV:C_{60} | I^-:I_3^-PEDOT | ITO solid state PECs, respectively.

In both cases photovoltage increased immediately when the cell was illuminated and remained constant during illuminations (Fig. 4.2.3) and it decayed slowly after stopping illumination to a dark potential of 20 mV for pure MDMO-PPV based PEC and to 10 mV for MDMO-PPV:C_{60} based PEC. The steady state photovoltage resulted by switching the illumination on is 198 and 150 mV for the pure MDMO-PPV and MDMO-PPV/C_{60} solid-state PEC devices, respectively.

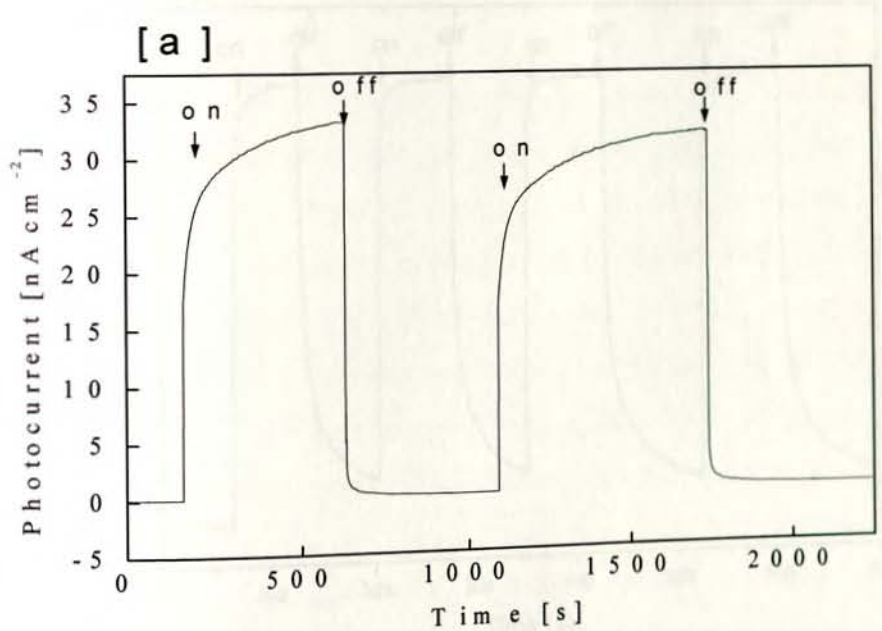

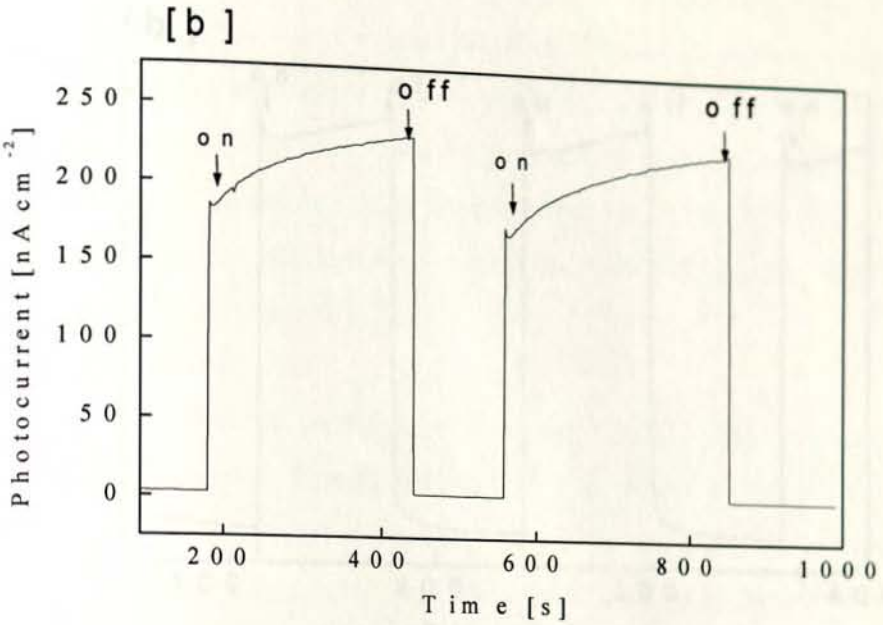

Fig. 4.2.2. Photocurrent response to switching illumination on and off from the front side of the solid-state PECs based on **[a]** pure MDMO-PPV & **[b]** MDMO-PPV/C_{60} blend.

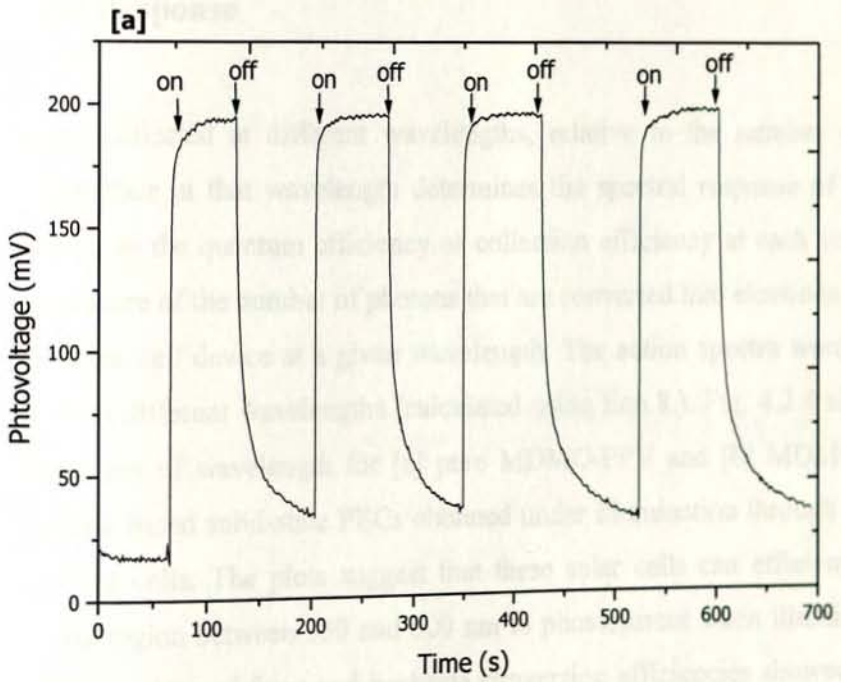

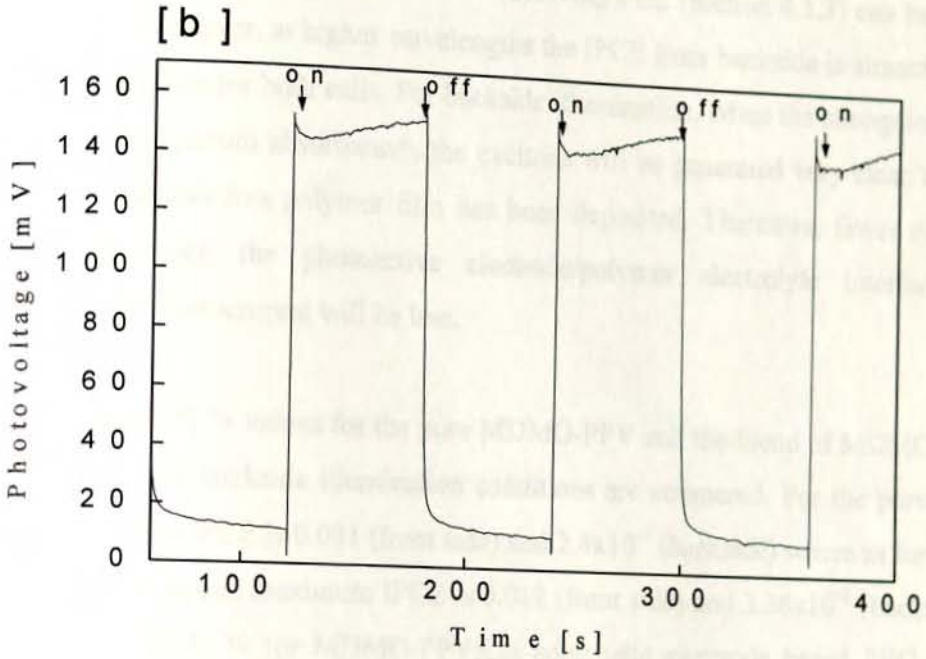

Fig. 4.2.3. Photovoltage response to switching illumination on and off from the front side of the solid-state PECs based on **[a]** pure MDMO-PPV & **[b]** MDMO-PPV/C_{60} blend.

4.2.3. Spectral Response

The photocurrent collected at different wavelengths, relative to the number of photons incident on the surface at that wavelength determines the spectral response of the device (sometimes known as the quantum efficiency or collection efficiency at each wavelength). The IPCE is a measure of the number of photons that are converted into electrons withdrawn as current by a solar cell device at a given wavelength. The action spectra were plotted in terms of IPCE % at different wavelengths (calculated using Eqn.8.). Fig. 4.2.4 shows IPCE % plotted as function of wavelength for [a] pure MDMO-PPV and [b] MDMO-PPV:C_{60} composite electrode based solid-state PECs obtained under illumination through front sides and backside of the cells. The plots suggest that these solar cells can efficiently convert visible light in the region between 350 and 600 nm to photocurrent when illuminated from the front side. Comparison of front and backside conversion efficiencies showed that front side illumination has greater IPCE than backside illumination at the maximum absorbance

for both cells. The same explanation as for P3HT/C_{60} PEC (section 4.1.3) can be given for this difference. However, at higher wavelengths the IPCE from backside is almost similar to those from front side for both cells. For backside illumination, when the absorption constant is high (at the maximum absorbance), the excitons will be generated very close to the ITO on which the photoactive polymer film has been deposited. Therefore, fewer numbers of excitons will reach the photoactive electrode/polymer electrolyte interface. As a consequence the photocurrent will be less.

The maximum IPCE % values for the pure MDMO-PPV and the blend of MDMO-PPV/C_{60} from front side and backside illumination conditions are compared. For the pure MDMO-PPV cell maximum IPCE is 0.001 (front side) and 2.4×10^{-5} (backside) where as for the blend of MDMO-PPV/C_{60} cell maximum IPCE is 0.012 (front side) and 3.36×10^{-3} (backside). The high values of IPCE % for MDMO-PPV:C_{60} composite electrode based PEC is due to greater photocurrent of the cell.

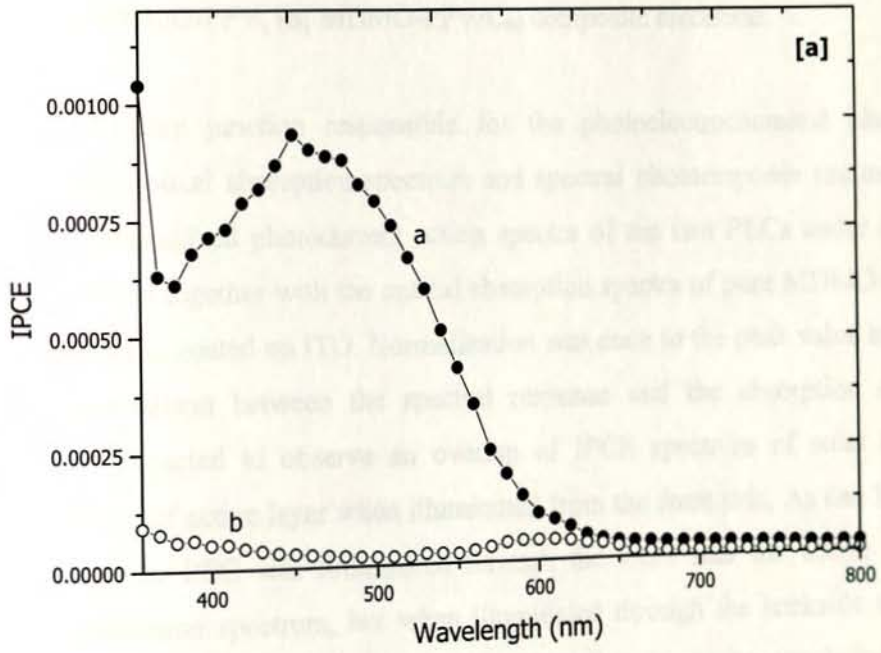

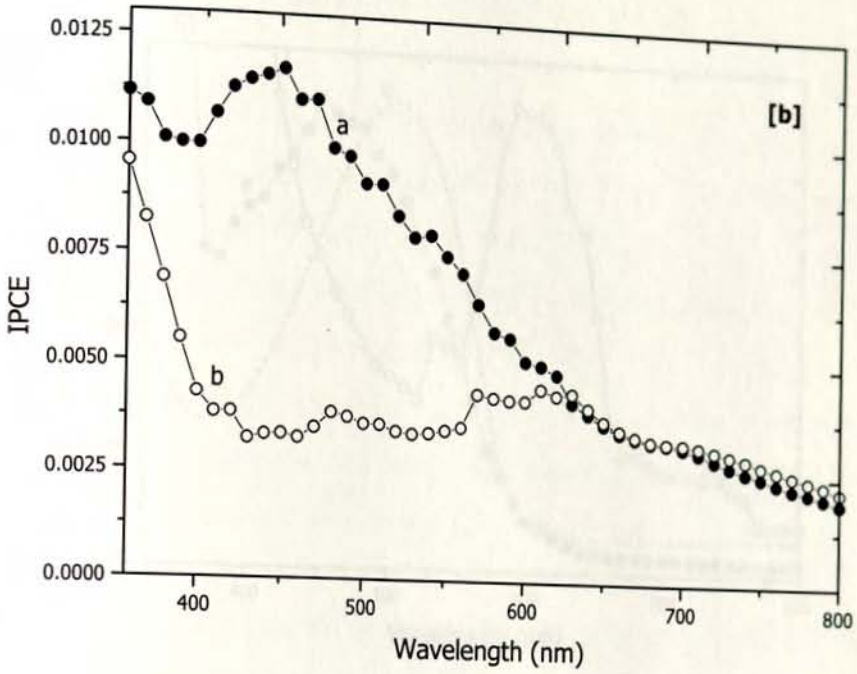

Fig. 4.2.4. Action spectrum of the all-solid-state PECs under a) front and b) backside illumination. **[a]** MDMO-PPV, **[b]** MDMO-PPV/C_{60} composite electrode.

To identify the active junction responsible for the photoelectrochemical phenomena, comparison of the optical absorption spectrum and spectral photoresponse are used. Fig. 4.2.5 shows the normalized photocurrent action spectra of the two PECs under front and backside illumination together with the optical absorption spectra of pure MDMO-PPV and MDMO-PPV with C_{60} coated on ITO. Normalization was done to the peak value in order to facilitate the comparison between the spectral response and the absorption spectrum. Actually, it was expected to observe an overlap of IPCE spectrum of solar cell with absorption spectrum of active layer when illuminated from the front side. As can be seen in both cases, when the PEC was illuminated through the front side the action spectrum resembles the absorption spectrum, but when illuminated through the backside the action spectrum and the absorption spectrum mismatch. Therefore it can be concluded that the junction responsible for the photocurrent was photoactive electrode/polymer electrolyte interface.

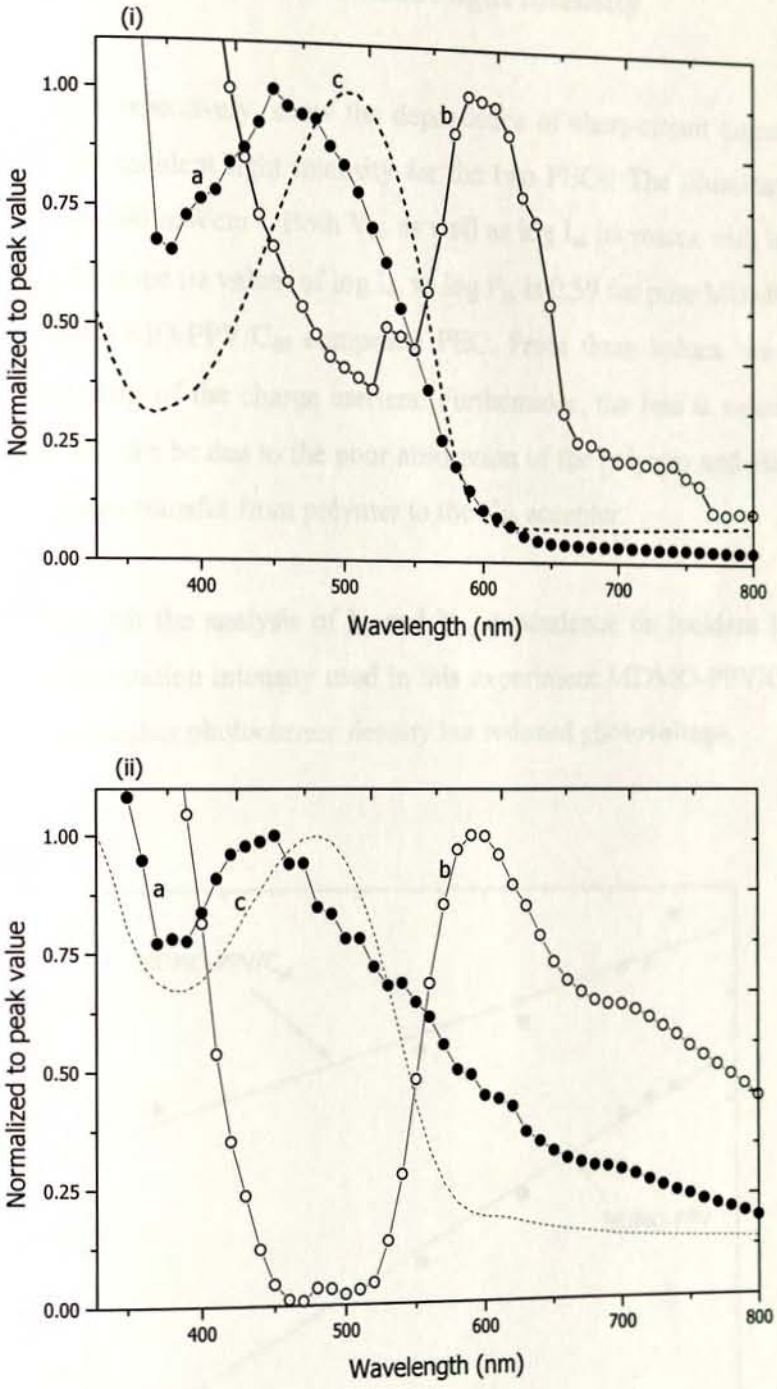

Fig. 4.2.5. Normalized photocurrent action spectrum of (i) pure MDMO-PPV and (ii) blend of MDMO-PPV/C_{60} for illumination through a) front side b) backside and c) optical absorption spectrum of MDMO- PPV and MDMO-PPV/C_{60} films on ITO normalized to the peak value.

4.2.4. V_{oc} and I_{sc} dependence on incident light intensity

Fig. 4.2.6 and 4.2.7, respectively, show the dependence of short-circuit current and open-circuit voltage on the incident light intensity for the two PECs. The illumination intensity was varied from 1 to 100 $mWcm^{-2}$. Both V_{oc} as well as log I_{sc} increases with increasing log P_{in} for each cell. The slope (α value) of log I_{sc} vs log P_{in} is 0.59 for pure MDMO-PPV based PEC and 0.52 for MDMO-PPV/C_{60} composite PEC. From these values, we can see that there is a recombination of the charge carriers. Furthermore, the less α value of MDMO-PPV/C_{60} based device can be due to the poor absorption of the polymer and other relaxation pathways beside charge transfer from polymer to the C_{60} acceptor.

It can be concluded that the analysis of I_{sc} and V_{oc} dependence on incident light intensity shows that at all illumination intensity used in this experiment MDMO-PPV/C_{60} composite based PEC exhibited higher photocurrent density but reduced photovoltage.

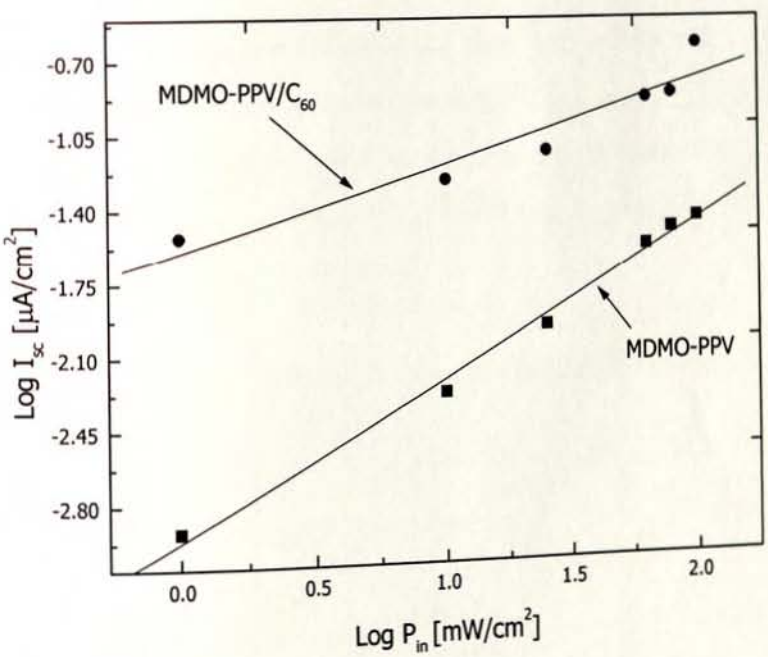

Fig. 4.2.6. Plot of log I_{sc} versus log P_{in} of ITO | MDMO-PPV:C_{60} | POMOE:I_3^-/I^- | PEDOT | ITO solid-state PEC.

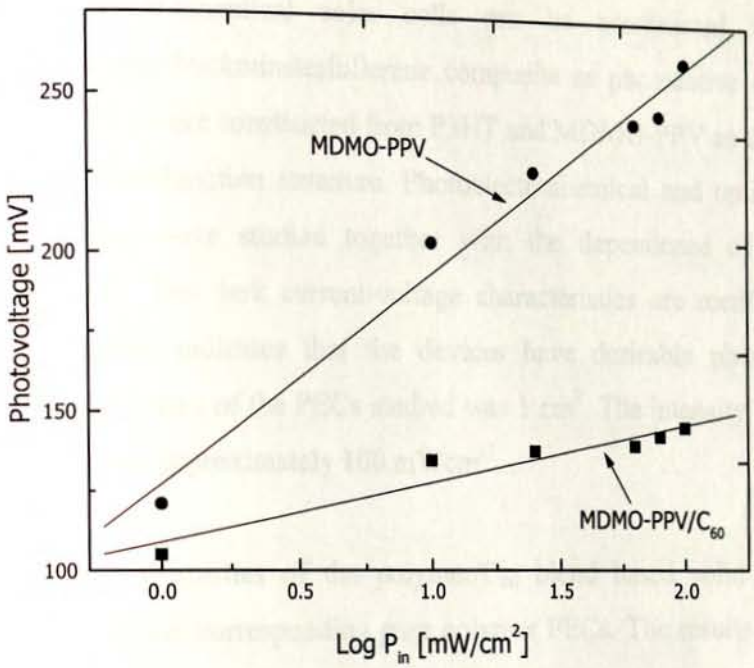

Fig. 4.2.7. Plot of V_{oc} versus log P_{in} of ITO | MDMO-PPV:C_{60} | POMOE:I_3^-/I^- | PEDOT | ITO solid-state PEC.

5. CONCLUSION

Solid state photoelectrochemical solar cells can be constructed with conjugated semiconducting polymer/buckminsterfullerene composite as photoactive electrode. In this study, solid-state PECs were constructed from P3HT and MDMO-PPV as donors, and C_{60} as acceptor, in bulk heterojunction structure. Photoelectrochemical and optical properties of these organic devices were studied together with the dependence of I_{sc} and V_{oc} on illumination intensity. The dark current-voltage characteristics are rectifying in both the devices studied, which indicates that the devices have desirable photoelectrochemical property. The effective area of the PECs studied was 1 cm^2. The intensity of the white light incident on the cell was approximately 100 $mWcm^{-2}$.

Photoelectrochemical properties of the polymer/C_{60} blend based solid-state PECs were compared with that of the corresponding pure polymer PECs. The results show that I_{sc} and IPCE % values were increased in many folds while the other measured PEC parameters were slightly less for polymer/C_{60} based PECs.

Table 4 summarizes the maximum values of the main solar cell parameters measured for the solid-state PECs whose active layer is composed of P3HT/C_{60} and MDMO-PPV/C_{60} blends. The conjugated semiconducting polymer/C_{60} stoichiometry is identical (1:1 w/w) in both the PECs studied. In addition, the active layer of both PECs is a smooth film indicating phase separation at most on the small dimensions.

Table 4. V_{oc}, I_{sc}, FF and IPCE % for the two solid-state PECs based on polymer/C_{60} blends for comparison.

Photoactive layer	V_{oc} (mV)	I_{sc} (μAcm^{-2})	FF	IPCE (%)
P3HT/C_{60} blend	97.8	7.28	0.26	0.43
MDMO-PPV/C_{60} blend	146	0.171	0.25	0.012

As can be seen from the table, there is considerable variation in V_{oc}, I_{sc}, FF and IPCE % between different polymers.

6. REFERENCES

1. H. J. Hovel, *Semiconductors and semimetals*, Vol. II, Solar Cells, academic press, New York, 1975.
2. H. Shirakawa, E. J. Louis, A.G. MacDiarmid, C.K. Chiang and A. J. Heeger, *J. Chem. Com.*, **16** (1977) 578.
3. J. Kaniki, *Handbook of conducting polymers*, ed. T. A. Skotheim, New York, Marcel Dekker, (1986).
4. W. Banikassegn and O. Inganas, *Thin Solid Films*, **293** (1997) 138.
5. G. Gustafsson, M. Sundberg, O. Inganas and C. Svensson, *J. Mol. Elect.*, **6** (1990) 105.
6. C. S. Kuo, F. G. Wakim, S. K. Sengupta and S. K. Tripathy, *Jpn. J. Appl. Phys.*, **33** (1994) 2629.
7. D. Braun and A. J. Heeger, *Appl. Phys. Lett.*, **58** (1991) 1982.
8. P. Dyreklev, G. Gustafsson, O. Inganas and H. stubb, *Solid State Comm.*, **82** (1992) 317.
9. G. Yu and A. J. Heeger, *J. Appl. Phys.*, **78** (1995) 4510.
10. L. S. Roman, M. Wendimagegn, L. A. A. Pettersson, M. R. Andersson and O. Inganas, *Adv. Mat.*, **10** (1998) 10.
11. Teketel Yohannes and O. Inganas, *Solar energy and Solar Cells.*, **51**(1998) 193.
12. Teketel Yohannes, and O. Inganas, *Synth. Met.*, **107** (1999) 97.
13. Teketel Yohannes and O. Inganas, J. *Electrochem. Soc.*, **143,** 2310; and references cited therein.
14. M. Adi, Teketel Yohannes and T. Solomon, *Solar Energy Materials and Solar Cells.*, **83** (2004) 301-310.
15. L. C. Chen, D. Godovsky, O. Inganas, M. Svensson and M. R. Anderson, *Adv. Mater.*, **12** (200) 1367.
16. J. J. M. Halls, C. A. Walsh, N. C. Greenham, E. A. Marseglia, R. H. Friend, S. C. Moratti, and A. B. Holmes, *Nature.*, **376** (1995) 498.
17. S. E. Shaheen, C. J. Brabec, F. Padinger, T. Fromherz, J. C. Hummelen, and N. S. Sariciftic, *Appl. Phys. Lett.*, **78** (2001) 841.

18. T. Lemma, *Photoelectrochemical Solar Energy Conversion*, M.Sc. Thesis, Addis Ababa University, Addis Ababa, 2004.

19. G. Zerza, C. J. Brabec, G. Gerullo, S. De Silvestri, and N. S. Sariciftic, *Synth. Met.*, **119** (2001) 637.

20. F. W. Billmeyer, *Textbook of polymer Science*, John Wiely & Sons, Inc., New York, (1971).

21. S. Roth, *One-Dimensional Metals*, VCH Publishing, Inc. New York, NY, (1995).

22. H. Naarmann, *Synth. Met.*, **17** (1987) 223.

23. B. Scrosati, *Prog. Solid State Chem.*, **18** (1988) 1.

24. A. O. Patil, A. J. Heeger, and F. Wudl, *Chem. Rev.*, **88** (1988) 183.

25. A. K. Bakhshi, *Bull. Mater. Sci.*, **18** (1995) 469.

26. W. R. Salenck, and J. L. Bredas, *Solid State Comm*, Vol. 92, **Nos. 1-2** (1994) 31.

27. G. P. Evans, *Advances in Electrochemical science and Engineering*, Vol. 1. VCH Verlagsgesell Schaft mbH, 1990.

28. Teketel Yohannes, *All-Solid-State Photoelectrochemical Solar Energy Conversion*, Ph.D. dissertations, Addis Ababa, 1997.

29. H. C. Longuet-Higgeins and L. Salem, *Proc. Roy. Soc.*A, **251** (1959) 172.

30. J. A. People and S.H. Walmsley, *Mol. Phys.*, 5 (1962) 15.

31. L. Salem, *The molecular Orbital Theory of Conjugated polymers*, Benjamin, New York, 1966.

32. N. Basescu, Z. X. Liv, D. Moses, H. Naarmann, and N. Theophilou, *Nature.*, **327** (1987) 403.

33. J. S. Russel, *Proc. Roy. Soc.*, **134** (1844) 150.

34. J. L. Bredas, R. R. Chance, and R. Silbey, *Mol. Crys.*, **77** (1981) 319.

35. J. L. Bredas, B. Themans, J. G. Fripiat, J.M. Andre and R. R. Chance, *Phys. Rev.* B., **26** (1982) 5843.

36. Y. Onodera, *Phys. Rev.* B., **30** (1984) 301.

37. J. L. Bredas, J. C. Scott, K. Yakushi and G. B. Street, *Phys. Rev.* B., **30** (1984) 1023.

38. A. J. Heeger, S. Kivelson, J. R. Schrieffer and W. P. Su, *Rev. mod. Phys.*, **60** (1988) 782.

39. A. B. Kaiser, Electronic properties of conjugated polymers, ed. H. Kuzmany M. Mehring, S. Roth, Heidelberg: Springer Verlag, (1987).
40. S. Kivlson, *Phys. Rev.* B., **25** (1982) 3798.
41. D. E. Fenton, J. M. Parker and P. V. Wright, *Polymer*, **14** (1973) 589.
42. M. B. Armand, *Solid State Ionics.*, **69** (1994) 309.
43. P. V. Wright, *Electrochim. Acta.*, **43** (1998) 1137.
44. J. Owen, C. Booth and C. Price, In *Comprehensive Polymer Science*, Pergamon Press: Oxford, 1989, Ch. 21.
45. A. Valee, S. Besner and J. Prudhomme, *Electrochim. Acta.*, **37** (1992)1579.
46. S. Neyetz and D. Brown, *Electrochim. Acta.*, **43** (1998) 1343.
47. T. Sreekanth, M. J. Reddy and U. V. Rao, *J. Power Sources,* **93** (2001) 268.
48. T. Takeoka, H. Ohno and E. Tsuchida, *Polymer for Advanced Technologies*, John Wiley & Sons: New York, 1993.
49. P. V. Wright, *J. Polym. Sci.*, **14** (1976) 955.
50. M. B. Armand, *Solid State Ionics.*, **9/10** (1983) 745.
51. Z. Gadjourova, Y. G. Andreev, D. P. Tunstall and P. G. Bruce, *Nature*, **412** (2001) 20.
52. W. Wieczorek, K. Such, Z. Florjanczyk and J. Przyluski, *Electrochim. Acta.*, **37** (1992) 565.
53. J. Li, and I. M. Khan, *Macromolecules*, **26** (1993) 4544.
54. S. Kohjiva, S.Takesako, Y. Ykeda and S. Yamashita, *Polym. Bull.*, **23** (1990) 299.
55. H. Ohno, *Electrochim. Acta.*, **37** (1992) 1649.
56. O. Inganäs, C. Carlberg and Teketel Yohannes, *Electrochim. Acta.*, **43** (1998) 1615.
57. J. R. Craven, R. H. Mobbs and J. R. M. Giles, *Makromol.Chem. Rapid Com.*, **7** (1986) 81.
58. M. Nekoomanesh, H. S. Nagae, C. Booth and J. R. own, *J. Electrochem. Soc.*, **139** (1992) 3046.
59. N. S. Sariciftci, L. Smilowitz, A. J. Heeger and F. Wudl, *Science*, **258** (1992) 1474.
60. G. Horowitz, *Adv. Mater.*, **2** (1990) 617.
61. A. K. Ghosh and T. Feng, *J. Appl. Phys.*, **49** (1978) 5982.
62. D. A Seanor, *Electrical properties of polymers*, Academic Press, New York, 1982.

63. T. A. Skotheim, S. W. Feldberg, and M. B. Armand, *J. Phys. Paris Colloq.*,**C3** (1983) 615.

64. B. O'Regan and M. Gratzel, *Nature*, **353** (1991) 737.

65. B. Kraabel, D. McBranch, N. S. Sariciftci, D. Moses and A. J. Heeger, *Phys. Rev.* B., **50** (1994) 18543.

66. D. Gebeyehu, C. J. Brabec, N. S. Sariciftci, D. Vangeneugden, R. Kiebooms, D.Vanderzande, F. Kienberger and H. Schindler, *Synth. Met.*, **125** (2001) 279.

67. I. H. Campbell, P. S. Davids, D.L. Smith, N. N. Barashkov and J. P. Ferraris, *Appl. Phys. Lett.*, **72** (1998) 1863.

68. Q. Pei, G. Zuccarello, M. Ahlskog and O. Inganas, *polymer*, **35** (1994) 1347

69. C. J. Brabec, N. S. Sariciftci and J. C. Hummelen, *Adv. Funct.Mater.*, **11** (2001)15.

70. V. D. Mihailetchi, P. W. M. Blom, J. C. Hummelen and M. T. Rispens, *J. Appl. Phys.*, **94** (2003) 6849.

DECLARATION

I, the undersigned, declare that this thesis is my original work and has not been presented for a degree in any other University and that all the sources of materials used for this thesis has been duly acknowledged.

Name: Ushula Mengesha

Signature: _____

This thesis has been submitted for examination with my approval as University advisor.

Name: Dr. Teketel Yohannes

Signature: _____

Place and Date of Submission: Department of Chemistry

Addis Ababa University

June 2005